Cytochrome *c* Peroxidase Binds Two Molecules of Cytochrome *c*: Evidence for a Low-Affinity, Electron-Transfer-Active Site on Cytochrome *c* Peroxidase†

Eric D. A. Stemp‡ and Brian M. Hoffman*,‡,§

Department of Chemistry and Department of Biochemistry, Molecular Biology and Cell Biology, Northwestern University, Evanston, Illinois 60208-3113

Received April 30, 1993; Revised Manuscript Received July 7, 1993®

ABSTRACT: We have studied the affinity and stoichiometry of binding of cytochrome *c* (C*c*) to zinc-substituted cytochrome *c* peroxidase [(ZnP)C*c*P], which is structurally and electrostatically equivalent to ferrous C*c*P. Transient absorption spectroscopy has been used to measure both the total quenching of the triplet-state (ZnP)C*c*P [^{3}(ZnP)C*c*P] by Fe^{3+}C*c* and the fraction of that quenching that is due to electron transfer (et). This redox quenching results in the formation of an intermediate (**I**) containing the zinc porphyrin π-cation radical [$(ZnP)^+$C*c*P] and Fe^{2+}C*c*. In titrations of (ZnP)C*c*P with Fe^{3+}C*c*(F) at low ionic strength, where F represents the fungal cytochromes *c* from *Candida krusei*, *Pichia membranefaciens*, or the yeast protein iso-1, the appearance of the et intermediate lags behind the total quenching, with appreciable formation of **I** occurring only for C*c* to C*c*P ratios > 1. This behavior results from the formation of a 2:1 complex, where one Fe^{3+}C*c*(F) binds to a high-affinity domain that exhibits strong quenching yet is et-inactive, while the second Fe^{3+}C*c*(F) binds to a low-affinity domain that allows efficient et quenching. At constant concentrations of both proteins, raising the ionic strength eliminates most of the et quenching but reduces the total quenching only minimally, confirming that et occurs preferentially at the low-affinity binding domain, which is the more sensitive to ionic strength. Analogous experiments also favor a 2:1 binding stoichiometry for horse C*c* [C*c*(horse)] at low ionic strength, with et quenching again proceeding much more favorably in the 2:1 complex than in the 1:1 complex, as with C*c*(F). However, the Fe^{3+}C*c*(horse) quenches only by electron transfer, unlike the C*c*(F). The decay of the triplet-state (ZnP)C*c*P or magnesium-substituted C*c*P [(MgP)C*c*P] was examined during titrations with Fe^{3+}C*c* to determine limits for the dissociation rate constant (k_{off}) for the complex. Fe^{3+}C*c*(horse) bound to the high-affinity domain in a 1:1 complex at low ionic strength is in rapid exchange, with $k_{off} > 50\ s^{-1}$, whereas Fe^{3+}C*c*(F) has $k_{off} < 200\ s^{-1}$. Both types of Fe^{3+}C*c* have $k_{off} > 10^4\ s^{-1}$ when they are bound to the low-affinity domain in a 2:1 complex, at both low and high ionic strengths. In contrast, when in the ferrous form, both types of C*c* have much lower values of k_{off} ($<10\ s^{-1}$) at low ionic strength when bound to the low-affinity domain. The low limit of k_{off} ($<200\ s^{-1}$) for Fe^{3+}C*c*(F) at low ionic strength indicates that a simple one-site mechanism cannot account for the much higher values found for the turnover number for C*c*(F:iso-1) [Erman, J. E., Kang, D. S., Kim, K. L., Summers, F. E., Matthis, A. L., & Vitello, L. B. (1991) *Mol. Cryst. Liq. Cryst. 194*, 253–258]. Confirming the proposal of Kang *et al.* [Kang, C. H., Ferguson-Miller, S., & Margoliash, E. (1977) *J. Biol. Chem. 252*, 919–926], a model of C*c*P function which accounts for all of these results includes two distinct binding domains for C*c*: a poorly reactive high-affinity domain with multiple, overlapping sites for C*c* and a highly reactive low-affinity domain elsewhere on the peroxidase.

Electron transfer (et)[1] within protein complexes is the subject of intense interest (Peerey *et al.*, 1991; Willie *et al.*, 1992; Zhou & Kostic, 1992a,b), with particular attention focused on the physiological complex formed between cytochrome *c* peroxidase (C*c*P) and the ubiquitous electron carrier, cytochrome *c* (C*c*) (Hazzard *et al.*, 1988a,b; Summers & Erman, 1988; Everest *et al.*, 1991; Geren *et al.*, 1991; Wallin *et al.*, 1991; Hahm *et al.*, 1992; McLendon & Hake, 1992). Although the primary function of C*c* may well be to shuttle electrons from cytochrome *c* reductase to cytochrome *c* oxidase in respiration (Pettigrew & Moore, 1987), X-ray quality crystals of these large, hydrophobic, membrane-bound proteins have not yet been obtained. In contrast, the crystal structure for the smaller, water-soluble C*c*P is known to high resolution (Finzel *et al.*, 1984). In part for this reason, the C*c*P–C*c* system has become a paradigm for protein–protein electron transfer in the far more complicated assemblies of respiration and photosynthesis.

Many previous studies of protein–protein interactions, including those between C*c*P and C*c* (Leonard & Yonetani, 1974; Ho *et al.*, 1985; Vitello & Erman, 1987; Corin *et al.*, 1991), have monitored complex formation and/or electron transfer through the quenching of a luminescent derivative of one of the partners by the other (Zhou & Kostic, 1992a; Simolo *et al.*, 1984). It is also common practice to use transient-absorption spectroscopy to study the kinetics of the appearance and disappearance of the intermediate resulting from et (Liang *et al.*, 1986; Wallin *et al.*, 1991; Zhou & Kostic, 1991, 1992b). We report here the first study that measures protein–protein *binding* both from the total quenching of zinc-substituted cytochrome *c* peroxidase [(ZnP)C*c*P] in the triplet state

† This work has been supported by the NIH (HL13531) and NSF (MCB 9207974).

‡ Department of Chemistry.

§ Department of Biochemistry, Molecular Biology and Cell Biology.

® Abstract published in *Advance ACS Abstracts*, September 1, 1993.

[1] Abbreviations: et, electron transfer; C*c*, cytochrome *c*; C*c*P, cytochrome *c* peroxidase; C*c*(F), fungal cytochrome *c*; (ZnP), zinc(II) protoporphyrin IX; (MgP), magnesium(II) protoporphyrin IX; (MP), metalloprotoporphyrin IX; C*c*P-I, compound I of C*c*P; C*c*P-II, compound II of C*c*P; KP_i, potassium phosphate; $(ZnP)^+$, zinc(II) porphyrin π-cation radical; ^{3}(ZnP), zinc(II) porphyrin triplet state; **I**, electron-transfer intermediate; μ, ionic strength.

0006-2960/93/0432-10848$04.00/0 © 1993 American Chemical Society

[^{3}(ZnP)CcP] by ferricytochrome *c* (Fe^{3+}Cc) and from a quantification of the electron-transfer quenching component through transient-absorbance studies of the intermediate formed by et within the complex [^{3}(ZnP)CcP,Fe^{3+}Cc]. This approach resolves the long-standing question concerning the stoichiometry with which CcP binds Cc, showing that at low ionic strength ($\mu < 50$ mM) the enzyme simultaneously binds two molecules of Fe^{3+}Cc at two distinct binding domains with widely different affinities and et activities.

The issue of binding stoichiometry is of particular concern with CcP because it catalyzes the *two*-electron reduction of hydrogen peroxide by successive reaction with *two* molecules of ferrocytochrome *c* [Fe^{2+}Cc] (Yonetani, 1976). The overall reaction is

$$2Fe^{2+}Cc + H_2O_2 + 2H^+ \rightarrow 2Fe^{3+}\ Cc + 2H_2O \quad (1)$$

Minimally, the catalytic cycle requires three steps, as shown in Scheme I. CcP first undergoes a two-electron oxidation by

Scheme I

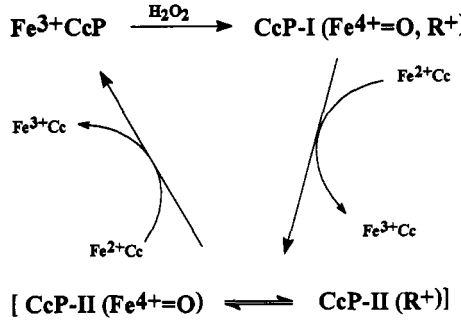

H_2O_2 to form an oxidized intermediate (CcP-I), usually called compound I or compound ES. The two oxidizing equivalents are stored as a ferryl iron–oxo species and as an amino acid radical (Bosshard *et al.*, 1991) of Trp-191 (Trp-191$^{\cdot}$) (Sivaraja *et al.*, 1989). In the next step of the catalytic cycle, a molecule of ferrocytochrome *c* reduces compound I by one electron to form a state, denoted compound II (CcP-II), which can carry the remaining oxidizing equivalent at either the heme iron or the radical. A stopped-flow investigation showed that the oxyferryl site is reduced first (Summers & Erman, 1988), so that reduction of the radical by a second molecule of Fe^{2+}Cc would appear to be the final step that restores the resting-state enzyme. However, electron transfer to Trp-191$^{\cdot}$ precedes reduction of the iron in studies of ruthenium-modified Fe^{3+}Cc in which the photoexcited ruthenium reduces the Cc heme iron, which in turn reduces the bound CcP-I (Geren *et al.*, 1991; Hahm *et al.*, 1992). The demonstration of internal et between the two sites in CcP-II further complicates the situation (Ho *et al.*, 1983, 1984). The fact that the catalytic cycle involves two cytochrome oxidation steps and two geometrically distinct redox centers within the peroxidase obviously leads to the question of whether CcP reacts with Cc at only one location, in which case the processes of binding and oxidizing two molecules of Cc are necessarily sequential, or whether there is more than one et-active domain.

CcP and Cc have isoelectric points of 5 and 10, respectively, and it has been known for over 2 decades that the two proteins interact primarily through electrostatic forces (Mochan, 1970). A computer model for the docking of a 1:1 electron-transfer complex was generated by Poulos and Kraut (1980) from the crystal structures of yeast CcP (Poulos *et al.*, 1980) and tuna heart Cc (Swanson *et al.*, 1977), and numerous binding studies have concluded that only 1:1 complexes are found in solution and suffice to describe functional activity (Mochan & Nicholls, 1971; Gupta & Yonetani, 1973; Leonard & Yonetani, 1974; Erman & Vitello, 1980; Vitello & Erman, 1987; Kim *et al.*, 1990; Corin *et al.*, 1991; Moench *et al.*, 1992). Although Brownian dynamics simulations suggested that Cc can occupy any of several sites on the peroxidase (Northrup *et al.*, 1988), many of the specific ionic interactions predicted by the Poulos–Kraut model have been supported by NMR (Satterlee *et al.*, 1987), chemical modification (Waldmeyer & Bosshard, 1985), and cross-linking studies (Bechtold & Bosshard, 1985), suggesting that the computer model does in fact approximate the dominant conformation of the complex in solution. Pelletier and Kraut (1992) recently solved the crystal structures for 1:1 complexes of CcP with yeast iso-1 Cc and horse Cc; these cocrystals reveal a binding site that is different from, *but* overlapping with, the putative Poulos–Kraut site and that is predicted to contain an efficient electron-transfer pathway (Beratan *et al.*, 1992).

Although the current consensus appears to favor a 1:1 binding stoichiometry, considerable evidence suggests that the thermodynamically most stable 1:1 electrostatic complex is not optimally configured for et and that rearrangement of the proteins within the complex is necessary for efficient et. Thus, at an equimolar Cc:CcP ratio, where it is universally agreed that only 1:1 binding is significant, et is inhibited at low ionic strength (Hazzard *et al.*, 1988b) but becomes more efficient when the ionic interactions are masked—either by increasing the ionic strength or through interface mutations on the cytochrome (Hazzard *et al.*, 1988a). Furthermore, the rate for et in a 1:1 cross-linked complex is less than the maximum rate for the noncovalent complex (Hazzard *et al.*, 1988b). These results all can be explained by conformational gating (Hoffman & Ratner, 1987; Hoffman *et al.*, 1990) of electron transfer through movement of Cc among several sites on the surface of CcP. Such a phenomenon also is observed for et from Fe^{2+}Cc to the π-cation radical of (ZnP)CcP [$(ZnP)^+$CcP] (Wallin *et al.*, 1991) and for the reaction of cytochrome *c* with plastocyanin (Peerey *et al.*, 1991; Zhou & Kostic, 1992a).

Furthermore, it has been proposed that the binding of CcP and Cc occurs with a 2:1 binding stoichiometry, which necessarily involves *nonoverlapping* binding *domains*. Thus, the formation of a 2:1 complex at low ionic strength was first demonstrated by size-exclusion chromatography (Kang *et al.*, 1977; Kornblatt & English, 1986), the first molecule binding with a high affinity and the second with a much lower affinity. Moreover, the steady-state kinetics with eukaryotic cytochrome *c* is biphasic at low ionic strength, with apparent K_M values similar to the directly determined K_d values, leading to a model of CcP with two catalytically active sites (Kang *et al.*, 1977). Furthermore, electrostatic calculations (Northrup *et al.*, 1988; Northrup & Thomasson, 1992) indicated that CcP can *accommodate* two cytochrome molecules without steric overlap by binding Cc at two distinct sites: a high-affinity site on the peroxidase corresponding to the putative Poulos–Kraut structure, and a low-affinity site near Asp-150 of CcP.

In this report, we investigate the binding and reactivity of both fungal and vertebrate cytochromes *c* with luminescent analogues of CcP [(MP)CcP] that contain either Zn porphyrin [(ZnP)CcP] or Mg porphyrin [(MgP)CcP] and that are structurally and electrostatically equivalent to the ferrous form of the native enzyme (Hoffman *et al.*, 1991). We first explore the binding of Cc by CcP through examination of the quenching of the triplet state of (MP)CcP [^{3}(MP)CcP] during titrations

with Fe^{3+}C*c*. These quenching measurements suggest that the interaction of Fe^{3+}C*c* with C*c*P involves a 2:1 stoichiometry under some conditions at least, and they further set limits on the dissociation rate constant, k_{off}, for the bound ferric cytochrome(s). The investigation of et-active binding through quantitation of the product of intracomplex ^{3}(ZnP)C*c*P → Fe^{3+}C*c* electron transfer includes a detailed consideration of the shape of the kinetic progress curves for the et intermediate, [(ZnP)$^+$C*c*P,Fe^{2+}C*c*] (**I**), produced by this reaction. This allows us to set an upper limit for the rate constant for dissociation of ferrous cytochrome *c* bound to (ZnP)$^+$C*c*P. Joint measurements of both triplet quenching and the yield of **I** make it possible to discriminate between productive and nonproductive binding of Fe^{3+}C*c* and to establish the relative degree to which quenching of ^{3}(MP)C*c*P is associated with (i) electron transfer or (ii) a nonredox quenching mechanism, presumably energy transfer.

These results definitively show that at low ionic strength (ZnP)C*c*P binds two Fe^{3+}C*c* at two distinct domains, one with high affinity and one with low affinity. Furthermore, just as the 1:1 complex of [C*c*P-I,Fe^{2+}C*c*] is strongly bound but does not exhibit optimal et under these conditions (Hazzard *et al.*, 1988a,b), so we also find that the high-affinity binding domain on (ZnP)C*c*P is far less et-active than the low-affinity domain. Furthermore, the dissociation rate constants for complexes of C*c*P with fungal Fe^{3+}C*c* at low ionic strength are much lower than the enzyme turnover number, suggesting that the low-affinity site offers an efficient et pathway to the oxyferryl heme of compound I and is important in the catalytic cycle of C*c*P.

EXPERIMENTAL PROCEDURES

Materials. D-Glucose, glucose oxidase (type X-S from *Aspergillus niger*), bovine liver catalase (thymol free), and G-25-150 Sephadex were purchased from Sigma Chemical Company. Potassium phosphate and potassium chloride were from Mallinkrodt. Porphyrins were from Porphyrin Products (Logan, UT). Potassium ferricyanide was from Aldrich Chemical Company. H_2O was obtained from a Milli-Q water purification system and typically had a resistivity of 14–18 MΩ·cm. Prepurified N_2 was from Matheson. Phosphate buffers were specifically chosen in order to be consistent with earlier work in our laboratory.[2]

Proteins. Cytochrome *c* peroxidase (C*c*P) was isolated from Red Star brand baker's yeast according to the protocol of Nelson *et al.* (1977), with improvements taken from recent procedures (English *et al.*, 1986; Smulevich *et al.*, 1989; Vitello *et al.*, 1990). Care was taken to remove bound acetate prior to crystallization, as suggested by Smulevich *et al.* (1989). The peroxidase gave a purity index (A_{408}/A_{280}) of 1.25–1.30 in 0.1 M potassium phosphate buffer (KP_i), pH 7; the presence of the charge-transfer band at 646 nm and a Soret/380 nm absorptivity ratio of 1.53 indicated that the protein is predominantly 5-coordinate, high-spin (Vitello *et al.*, 1990). The enzyme was stored as a crystalline suspension at 77 K in H_2O.

Preparation of metal-substituted cytochrome *c* peroxidase, (MP)C*c*P, was accomplished using a modification of Yonetani's method (1967), which will be published elsewhere.[3]

Concentrations of (ZnP)C*c*P and (MgP)C*c*P were determined from a Soret extinction coefficient of 196 mM^{-1} cm^{-1}.[4] The luminescent peroxidase derivatives were handled in the dark.

Cytochromes *c* from horse heart and *Candida krusei* were types VI and VII purchased from Sigma Chemical Company. Cytochrome *c* from *Pichia membranefaciens* is now offered by Sigma as a substitute for *C. krusei* C*c*. All fungal C*c* behave in a similar manner in our system. We chose *P. membranefaciens* and *C. krusei* C*c* as the representative fungal C*c* for extensive study, because they are readily available and they do not share the problems of interprotein disulfide formation and autoreduction associated with the reactive cysteine at position 102 of iso-1 C*c*. To confirm the validity of this strategy, some measurements were performed with recombinant *Saccharomyces cerevisiae* iso-1(C102T) cytochrome *c*, which is not susceptible to such problems (Cutler *et al.*, 1987); this protein was the generous gift of Prof. A. Grant Mauk. Although technically a mutant, the C102T modification is functionally insignificant, and this protein will simply be designated C*c*(F:*iso-1*) in this article. When discussing features common to all fungal cytochromes *c*, we use the notation C*c*(F) and add the name when necessary; for example, C*c*(F:*Ck*) denotes the fungal C*c* from *C. krusei*. All of the commercial cytochromes *c* were purified on CM52 resin (Whatman) by the method of Brautigan *et al.* (1978) or a slight modification thereof. Cytochromes *c* were typically oxidized immediately prior to use with an excess of potassium ferricyanide or NH_4[Co(dipicolinate)$_2$]. Excess oxidant was removed either by gel filtration or by extensive washing on CM52 resin prior to elution. Concentrations of the ferricytochromes were determined from a Soret extinction coefficient of 106 mM^{-1} cm^{-1} (Margoliash & Frohwirt, 1959).

Sample Preparation. Samples for flash photolysis were prepared in Pyrex or quartz optical cells closed with a stopcock. The buffer of choice was deoxygenated by gentle flushing with N_2 for about 30 min and added to the cell under positive nitrogen pressure with gas-tight syringes (Hamilton). Anaerobicity was ensured by including an enzymatic oxygen scavenging system in the sample: glucose oxidase (20 μg/mL), catalase (5 μg/mL), and glucose (10–20 mM). Finally, an aliquot of (MP)C*c*P was added, typically yielding a peroxidase concentration of ~5 μM. After the intrinsic lifetime of the ^{3}(MP)C*c*P was measured, small volumes of ferricytochrome *c* in the same buffer were syringed into the cell. In experiments where the purpose was to obtain a binding profile, the total volume of cytochrome *c* added was such that the sample dilution was no more than 10%.

Instrumentation. Optical spectra were recorded with a single beam, diode array spectrophotometer (Hewlett-Packard 8451). Excited states of the luminescent peroxidases were normally produced by irradiating the sample with a Q-switched, frequency-doubled Nd:YAG YG660A laser (Continuum). The laser typically delivered 40–80 mJ/pulse with a 7-ns pulse width. Other actinic sources included a Vivitar 285HV camera flash and a locally constructed xenon flash. The flash photolysis apparatus was of the conventional 90° design and will be described in detail elsewhere. Signal averaging was used to attain the desired signal/noise ratio. Triplet decay data required 1–25 transients, while the data for the electron-transfer intermediate typically involved 64–225 transients and 225–400 transients for the slow and fast kinetic phases, respectively (*vide infra*). The digitized transients were transferred to an IBM-compatible computer

[2] Although C*c* binds phosphate (Pettigrew & Moore, 1987), we chose KP_i buffers for consistency with our earlier work on (ZnP)C*c*P in this buffer system. An investigation of the C*c*P–C*c* binding interaction as a function of buffer identity is planned.

[3] Stemp, E. D. A., Nocek, J. M., Wallin, S. A., Siegel, D., Mansueto, L., & Hoffman, B. M., manuscript in preparation.

[4] Luchi, J., & Hoffman, B. M., manuscript in preparation.

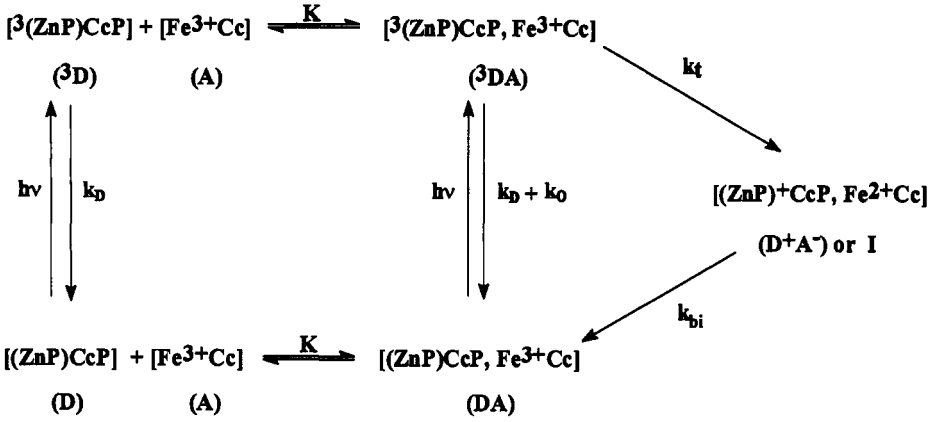

FIGURE 1: Photoinitiated electron-transfer cycle for the complex [(ZnP)C*c*P,Fe^{3+}C*c*].

and fit with the Marquardt nonlinear least-squares algorithm (Bevington, 1969).

Triplet Quenching Measurements. The lifetime of the (MP)C*c*P triplet state is readily monitored by transient-absorbance measurements at 475 nm, where the absorbance change is due almost exclusively to the triplet–ground color change (Liang *et al.*, 1988).[3] The intrinsic decay rate constant, k_D, measured for [^{3}(MP)C*c*P,Fe^{2+}C*c*] is identical to that for ^{3}(MP)C*c*P in the absence of C*c*, indicating that Fe^{2+}C*c* does not quench the triplet. Addition of Fe^{3+}C*c* decreases the triplet lifetime. When the rate constant for complex dissociation, k_{off}, is greater than the observed decay constant, k_{obs}, the triplet decay is exponential for any ratio of cytochrome to peroxidase, and the measured quenching contribution, k_q, is given by

$$k_q = k_{obs} - k_D \quad (2)$$

Reported values of k_q in this article represent the average of 2–10 measurements and have an error of ± 5 s^{-1}. Note that in Figure 1, k_q is the sum of all triplet quenching pathways and may be written as

$$k_q = k_t + k_o \quad (3)$$

where k_t is the photoinitiated et rate constant and k_O is the rate constant for nonredox quenching. We denote the decay constant for the *fully bound* complex as k_p ($=k_{plateau}$).

For 1:1 binding in this rapid-exchange limit, the measured quenching constant at any point in a titration is given by

$$k_q = k_Q y = k_Q [([CcP]_t + [Cc]_t + K_d) - \sqrt{([CcP]_t + [Cc]_t + K_d)^2 - 4[CcP]_t[Cc]_t}]/2[CcP]_t \quad (4)$$

where y is the fraction of C*c*P sites that are occupied, k_Q is the intracomplex quenching constant, K_d is the equilibrium dissociation constant, and $[CcP]_t$ and $[Cc]_t$ are the *total* concentrations of peroxidase and cytochrome *c*, respectively. Although the "site 1" on C*c*P in fact is a domain containing multiple sites (see above and Figure 10 below), for simplicity we ignore this throughout the Results section.

If (MP)C*c*P independently binds C*c* at two nonoverlapping sites with fixed but different affinities and with quenching constants ^1k_Q and ^2k_Q, then in this fast-exchange limit the observed quenching constant is given by

$$k_q = {}^1k_Q {}^1y + {}^2k_Q {}^2y \quad (5a)$$

where ^1y and ^2y are the fractions bound for sites 1 and 2, irrespective of stoichiometry. The relationship of the site binding constants and so-called stoichiometric constants is clarified in Scheme II, which follows Klotz (Klotz & Hunston, 1979; Klotz, 1985) in depicting all four possible states of the system with an overall 2:1 binding stoichiometry. Here, D and A denote C*c*P and C*c*, respectively; K denotes the equilibrium constant. In the scheme, superscripts to the left of D or K refer to the site number, and subscripts to the right of A or K designate the stoichiometry. For example, the term $^{2,1}K_2$ is the *site* constant for binding of A to site 1 of D with site 2 previously occupied by one A molecule. Below the scheme, the stoichiometric conversion of D to DA_2 is depicted; for example, $[DA_1] = [^1DA_1] + [^2DA_1]$. In the text of this article we add a subscript d to emphasize our use of dissociation constants. An alternate, more general form for k_q then is

$$k_q = {}^1k_Q\left(\frac{[^1DA_1] + [DA_2]}{[CcP]_t}\right) + {}^2k_Q\left(\frac{[^2DA_1] + [DA_2]}{[CcP]_t}\right) \quad (5b)$$

where $[^1DA_1]$ and $[^2DA_1]$ are the concentrations of 1:1 complex where C*c*(A) is bound at sites 1 and 2 of C*c*P(D), respectively (Scheme II). A complete description of the 2:1 binding eqs will be given elsewhere.[5]

Scheme II

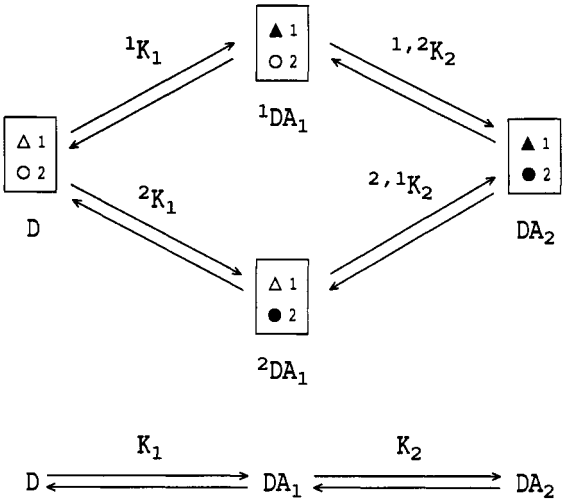

Below we show that the binding of Fe^{3+}C*c* is much stronger to site 1 than to site 2. In this case, the stoichiometric constants K_{d1} and K_{d2} equal the site constants $^1K_{d1}$ and $^{1,2}K_{d2}$, respectively, and sites 1 and 2 are filled sequentially during a titration with Fe^{3+}C*c*. In the simplified model where the two sites have fixed affinities, we may define simplified symbols: $^{1,2}K_{d2} = {}^2K_{d1} \equiv {}^2K_d$ and $^{2,1}K_{d2} = {}^1K_{d1} \equiv {}^1K_d$. Unless

[5] Zhou, J., & Hoffman, B. M., unpublished results.

stated otherwise, we will use the terms ^1K_d and ^1k_Q to denote the binding and quenching constants at site 1 for fits of titration data both to the 1:1 binding isotherm (eq 4) and to the 2:1 isotherm (eq 5a).

In the slow-exchange limit of a 1:1 complex, where $k_{off} < k_{obs}$, the ^{3}(MP)C*c*P decay during a titration would be biexponential:

$$[^3(MP)CcP]_t = [^3(MP)CcP]_o[(1-y)e^{-k_D t} + ye^{-k_p t}] \quad (6)$$

where y again is the fraction of (MP)C*c*P that carries a bound C*c*, k_D is the intrinsic decay rate constant, and k_p is again the intracomplex decay rate constant at saturation. For a titration of a system in this regime, eq 4 can be used to obtain the binding constant if one replaces k_q with y and sets $k_Q = 1$. When $k_{off} \approx k_{obs}$ in a 1:1 complex, the decay again will be nonexponential, typically a biexponential where the rate constants cannot be simply assigned to complexed and free ^{3}(MP)C*c*P, respectively (Hoffman & Ratner, 1987; Hoffman *et al.*, 1990). Because the intrinsic triplet decay constant (k_D) is much smaller for (MgP)C*c*P than for (ZnP)C*c*P, the former is better suited for studying cytochromes for which the quenching term, k_q, is small.

Kinetics for the Electron-Transfer Intermediate, I. Electron transfer within the excited precursor complex, [^{3}(ZnP)-C*c*P,Fe^{3+}C*c*], leads to formation of the electron-transfer intermediate, **I**, which we write as [$(ZnP)^+$C*c*P,Fe^{2+}C*c*] to denote the π-cation radical and ferroheme redox centers, irrespective of whether a second Fe^{3+}C*c* may be present (Wallin *et al.*, 1991). The concentration of this et intermediate therefore reflects the extent of binding in the triplet state. The observed progress curves for **I** were fit to a multiphasic expression of

$$A_t = \beta\sum g_i\left(\frac{e^{-k_{obs}t} - e^{-k_{bi}t}}{k_{bi} - k_{obs}}\right) + A_J e^{-k_{obs}t} \quad (7)$$

where g_i is the fractional weight of phase i, k_{bi} is the intracomplex, $Fe^{2+}Cc \rightarrow (ZnP)^+$C*c*P et rate constant for phase i, and the term A_J accounts for departures from the triplet–ground isosbestic. If ^{3}(ZnP)C*c*P transfers electrons with a rate constant k_t to an Fe^{3+}C*c* bound at a single site, then the factor β is given by

$$\beta = \beta_j = \Delta\epsilon_\lambda {}^3D(0)k_t y \quad (8)$$

where, again, y is the et-active site occupancy, $\Delta\epsilon_\lambda$ is the difference in extinction coefficients of **I** and ground at wavelength λ, and ^{3}D(0) is the initial concentration of ^{3}(ZnP)C*c*P produced by the actinic flash.[6]

For fixed ^{3}D(0), the maximum absorbance (A_{max}) for **I**, as described by eqs 7 and 8, increases monotonically with the fraction of ^{3}(ZnP)C*c*P bound in a complex, y. However, the increase is not linear, despite the fact that $A(t) \propto \beta \propto y$. This occurs because k_{obs} changes with y (e.g., eq 4), and thus the shape and height of the absorbance transient for **I** (eq 7) necessarily change somewhat during a titration; however, it is shown that these effects are minimal for the present study (Figures 6 and 7). As a result, this maximum absorbance for **I** gives a reliable measure of y during titration, provided one compensates for decreases in ^{3}D(0) caused by (i) inner filter effects from the strongly absorbing C*c*, (ii) singlet quenching, and (iii) dilution. This is done by normalizing A_{max} with respect to the ^{3}(ZnP)C*c*P transient absorbance difference, $\Delta A(0)$, which also is proportional to ^{3}D(0). This absorbance difference is measured at 475 nm, where the intermediate contributes negligibly to the absorbance change. We employ the normalized quantity, [**I**], as a model-independent parameter whose contribution from et to C*c* is proportional to k_t, and which increases monotonically with the fractional binding of C*c* to ^{3}(ZnP)C*c*P, y:

$$[\mathbf{I}] = A_{max}(549\text{ nm})/\Delta A(t=0, 475\text{ nm}) \quad (9)$$

A true quantum yield for formation of **I** can be derived from a progress curve for this intermediate upon assuming a kinetic model.

RESULTS

This section begins with a brief summary of the quenching process and the electron-transfer cycle for the [(ZnP)-C*c*P,Fe^{3+}C*c*] system. This is followed by a detailed examination of the progress curves both for ^{3}(MP)C*c*P in the presence of C*c* and for the et intermediate; this yields limits on the rate constants for dissociation of the cytochrome from the peroxidase in states DA and **I** (Figure 1). Quenching titrations are then used to explore the binding of C*c* to C*c*P at pH 7, including the influence of cytochrome type and buffer concentration. Indications of a 2:1 stoichiometry are then confirmed by a combined study of the changes in quenching and in the amount of et intermediate formed during titration of (ZnP)C*c*P with Fe^{3+}C*c*. This is followed by a complementary experiment, a "reverse" titration in which the preformed complex is dissociated by raising the ionic strength. Finally, the influence of pH and [P_i] on binding is examined in greater detail in titrations of (ZnP)C*c*P with Fe^{3+}C*c*(horse), and the binding constants obtained from quenching titrations are discussed.

Quenching and et Scheme for [ZnCcP,FeCc]. Figure 1 depicts the electron-transfer cycle for the [(ZnP)C*c*P,C*c*] system, complete with binding equilibria appropriate for a 1:1 binding stoichiometry; extension to a 2:1 complex is straightforward. Photoexcitation of ground-state (ZnP)C*c*P (D) leads to formation of the singlet state (not shown), which rapidly undergoes intersystem crossing to form the triplet state (^{3}D). In the absence of Fe^{3+}C*c*, ^{3}D decays exponentially with an intrinsic decay constant, k_D ($\approx$120 s^{-1} for ^{3}(ZnP)C*c*P). Both ground-state (ZnP)C*c*P and excited-state ^{3}(ZnP)C*c*P bind Fe^{3+}C*c* to form the complexes DA and ^{3}DA, respectively. As there is neither a change in charge nor metal ion coordination upon excitation from D to ^{3}D, we may take the binding constants for Fe^{3+}C*c* to be identical in the ground and triplet states of (ZnP)C*c*P and thus do not distinguish between them in Figure 1 or below. The complex ^{3}DA can decay directly to ground with a rate constant, ($k_D + k_Q$), where k_Q is the rate constant for nonredox quenching. Alternatively, the $^3D \rightarrow A$ intracomplex electron-transfer reaction can occur with a rate constant k_t to give the charge-separated intermediate, D^+A^-, denoted **I**. Because **I** is formed from the excited precursor complex ^{3}DA, the concentration of **I** reflects the extent of binding in the triplet state, formally through the coefficient β (eq 8) and empirically through the absorbance maximum (eq 9). The et reaction to regenerate DA is multiphasic (Wallin *et al.*, 1991) and is described by eq 7.

In the [(ZnP)C*c*P,C*c*] system, photoinitiated et proceeds from the porphyrin triplet state to the ferriheme of C*c*, and the cycle is closed with et from the ferroheme to the porphyrin-based, π-cation radical ($(ZnP)^+$C*c*P). Because Trp-191$^\cdot$ is not formed, our system is not complicated by two competing et processes at two separate redox centers in C*c*P. Although the photoinitiated et event proceeds in the reverse direction

[6] For transfer at multiple sites, $\beta = \sum\beta_j = \Delta\epsilon_\lambda {}^3D(0)\sum_j {}^jk_t {}^jy$, where each site is characterized by ^jk_t and ^jy.

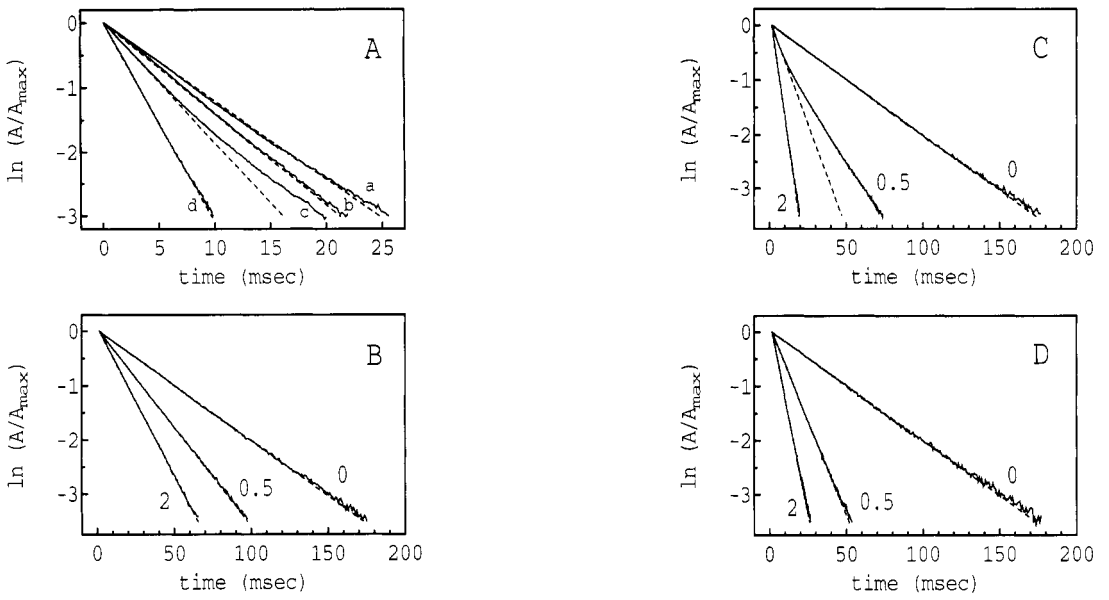

FIGURE 2: ^{3}(MP)C*c*P progress curves monitored at 475 nm during quenching titrations with Fe^{3+}C*c*. (A) Semilog plots of ^{3}(ZnP)C*c*P decays in 1 mM KP_i (pH 7). Solid lines represent data for (a) ^{3}(ZnP)C*c*P uncomplexed, (b) at C*c*/C*c*P = 1.2 with Fe^{3+}C*c*(horse), (c) at C*c*/C*c*P = 0.44, and (d) at 6.5 with Fe^{3+}C*c*(F:*Pm*). Dashed lines are single-exponential fits with k_{obs} = 124, 136, and 312 s^{-1} for decays a,b, and d, respectively; decay c is well-described by a biexponential decay (eq 6) where k_1 = 298 s^{-1}, k_2 = 123 s^{-1}, and f_1 = 0.48. The dashed line with c is a single-exponential fit to the initial 10% of the decay. (B) Semilog plots of ^{3}(MgP)C*c*P decays during a titration with Fe^{3+}C*c*(horse) in 10 mM KP_i (pH 7). From right to left, solid lines represent data for C*c*/C*c*P = 0, 0.61, and 2.37, for which single-exponential fits (dashed lines) gave k_{obs} = 21, 37, and 55 s^{-1}, respectively. (C) Semilog plots of ^{3}(MgP)C*c*P decays during a titration with Fe^{3+}C*c*(F:*Pm*) in 10 mM KP_i (pH 7). From right to left, solid lines represent data for C*c*/C*c*P = 0, 0.55, and 2.20. Single-exponential fits (dashed lines) gave k_{obs} = 21 and 200 s^{-1} for free and complexed ^{3}(MgP)C*c*P, respectively. The decay at C*c*/C*c*P = 0.55 is well-described by a biexponential function where k_1 = 175 s^{-1}, k_2 = 44 s^{-1}, and f_1 = 0.39; the dashed line is the same as in decay c of A. (D) Semilog plots of ^{3}(MgP)C*c*P decays during a titration with Fe^{3+}C*c*(F:*Pm*) in 50 mM KP_i (pH 7). From right to left, solid lines represent data for C*c*/C*c*P = 0, 0.54, and 2.25, for which single-exponential fits gave k_{obs} = 21, 70, and 144 s^{-1}, respectively.Conditions: $[(MP)CcP]_0 = 5 \pm 0.5$ μM; 20 °C.

of the physiological reaction, the corresponding thermal et reaction from Fe^{2+}C*c* to (ZnP)$^+$C*c*P parallels the flow of electrons *in vivo* and is analogous to et from Fe^{2+}C*c* to C*c*P-II(Fe^{4+}=O). Furthermore, the majority of this process proceeds with a rate constant of ~3000 s^{-1} (Wallin *et al.*, 1991), comparable to the rate constants for the Fe^{2+}C*c* → compound I et reaction (Hazzard *et al.*, 1988a,b).

*Triplet Decay Curves and Rate Constants for Dissociation of Fe^{3+}C*c* from C*c*P. (1) C*c*(horse).* We reported earlier that the decay of ^{3}(ZnP)C*c*P in 10 mM KP_i (pH 7) is exponential throughout a quenching titration by Fe^{3+}C*c*(horse) (Ho *et al.*, 1985). Indeed, in all buffers where $[P_i] > 1$ mM and $6 \leq pH \leq 8$, ^{3}(ZnP)C*c*P decay traces remain exponential during a titration with Fe^{3+}C*c*(horse) over the range C*c*/C*c*P = 0–10 ([(ZnP)C*c*P] ≈5 μM). As an example, Figure 2A shows a semilog plot of the decay traces for ^{3}(ZnP)C*c*P in 1 mM KP_i (pH 7); the decay is linear in the absence of C*c* (decay a) and at a 1:1 ratio with Fe^{3+}C*c* (horse) (decay b). However, it is also clear that the addition of 1 equiv of Fe^{3+}C*c*(horse) leads to only a small increase in the ^{3}(ZnP)C*c*P decay constant, from k_{obs} = 123 to 136 s^{-1}, and it is not really possible to determine whether the quenching contribution is characterized by an exponential or a biexponential in such a case.

To clarify this situation, we repeated the experiment using (MgP)C*c*P, which has a substantially smaller decay constant, $k_D \approx 20\ s^{-1}$, but comparable triplet quenching by Fe^{3+}C*c*. The triplet decays again are exponential throughout a titration of (MgP)C*c*P with Fe^{3+}C*c*(horse) for $[P_i] \geq 1$ mM, as seen in Figure 2B for an experiment that employed 10 mM KP_i (pH 7). At C*c*/C*c*P values of 0, 0.5, and 2, the decays remain exponential as the triplet decay constant increases from k_D = 20 s^{-1} to k_{obs} = 55 s^{-1}. These results for the quenching of ^{3}(MgP)C*c*P indicate that the dissociation rate constant for the complex with Fe^{3+}C*c*(horse) obeys the inequality, $k_{off} > k_{obs} > \sim 50\ s^{-1}$, even at buffer concentrations as low as 1 mM KP_i, consistent with the fast exchange seen by NMR (Satterlee *et al.*, 1987; Moench *et al.*, 1992).

*(2) C*c*(F:Pichia membranefaciens) [C*c*(F:Pm)].* The quenching behavior of the fungal C*c* from *P. membranefaciens* is much different from that of C*c*(horse). In pH 7 buffers where $1 \leq [P_i] \leq 10$ mM, the decay of ^{3}(ZnP)C*c*P becomes nonexponential upon the addition of substoichiometric concentrations of Fe^{3+}C*c*(F:*Pm*) (decay c), but returns to exponential in the presence of excess C*c* (decay d), as illustrated in Figure 2A for 1 mM KP_i. The limiting case of slow exchange applies here, because the decays at C*c*/C*c*P < 1 can be described by a biexponential, where the slower rate constant is $k_D(^3(ZnP)CcP)$ = 123 s^{-1} and the faster rate constant corresponds to the intracomplex decay constant of $k_p = k_D + {}^1k_Q$ = 298 s^{-1} (eq 6). This suggests that, in 1 mM KP_i (pH 7), the residence time for Fe^{3+}C*c*(F:*Pm*) on the peroxidase is longer than the ^{3}(ZnP)C*c*P lifetime, i.e., $k_{off} < 120\ s^{-1}$ for Fe^{3+}C*c*(F:*Pm*), a result in agreement with an earlier study with C*c*(F:iso-2) (Ho *et al.*, 1985). The return to exponentiality at high C*c*/C*c*P further indicates that the biexponential behavior at low [C*c*] is not simply due to some trivial effect, such as photolytic degradation of the sample during the experiment.

During a titration of (MgP)C*c*P with Fe^{3+}C*c*(F:*Pm*) in 10 mM KP_i (pH 7) (Figure 2C), the decay is again biexponential at substoichiometric concentrations of C*c*. However, the slower rate constant does not simply correspond to that for free ^{3}(MgP)C*c*P, with k_D = 20 s^{-1}, which indicates that a simple limiting case of slow dissociation does not apply. Instead, dissociation of the (MgP)C*c*P complex with Fe^{3+}C*c*(F:*Pm*) in 10 mM KP_i (pH 7) is characterized by $20\ s^{-1} = k_D < k_{off} < k_{obs} = 200\ s^{-1}$. At saturating concentrations of

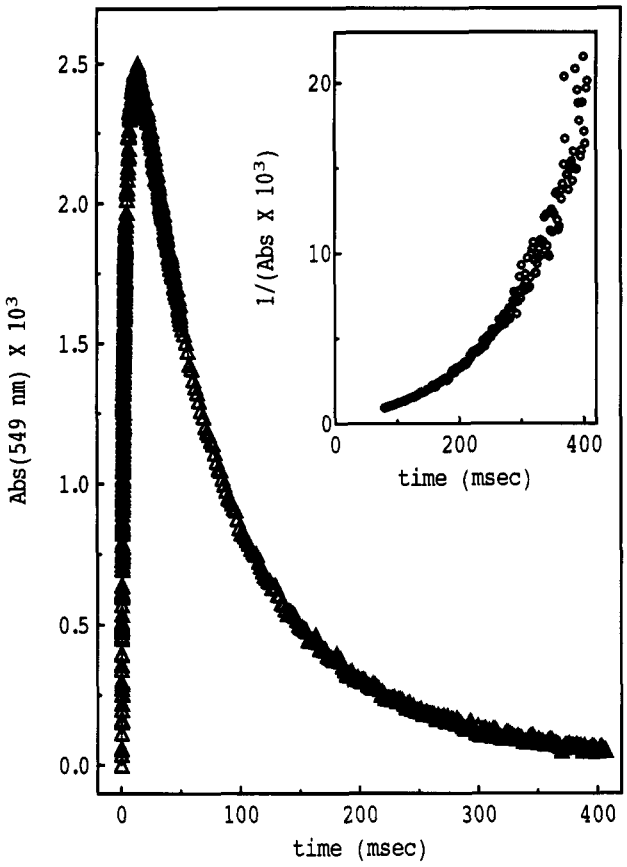

FIGURE 3: Kinetic progress curve at 549 nm for electron-transfer intermediate, I, formed upon flash photolysis of the [(ZnP)-CcP,Fe³⁺Cc(horse)] complex. Inset: Reciprocal of absorbance values plotted for $t > 80$ ms. Conditions: 4.6 μM (ZnP)CcP; 50 μM Fe³⁺Cc(horse) in 10 mM KP_i (pH 7); 20 °C.

cytochrome, the decay is once more exponential. Biexponential decays at Cc/CcP < 1 are seen with the other fungal cytochromes, Cc(F:*Ck*) and Cc(F:iso-1), which indicates that these cytochromes also have $k_{off} < 200$ s^{-1}.

At yet higher buffer concentrations, $[P_i] \geq 50$ mM, decay traces for ^{3}(MP)CcP (M = Zn, Mg) remain exponential throughout a titration with Fe³⁺Cc(F:*Pm*), as illustrated for ^{3}(MgP)CcP in 50 mM KP_i (pH 7) (Figure 2D). This indicates that the cytochrome undergoes a rapid association equilibrium in this medium and that $k_{off} > k_{obs} \approx 200$ s^{-1} at these ionic strengths. This is true for complexes of (MP)CcP with all of the cytochromes, both fungal and vertebrate, we have studied thus far.

Characteristics of the Electron-Transfer Intermediate, I. Triplet quenching is in part associated with the ^{3}(MP)CcP → Fe³⁺Cc et process within the excited-state (^{3}DA) complex. The full progress curve of the resulting [(MP)⁺CcP,Fe²⁺Cc] electron-transfer intermediate, called I in Figure 1, can be obtained by monitoring the absorbance change at a triplet–ground isosbestic point; this typically involves the ^{3}(ZnP)CcP–(ZnP)CcP isosbestic at 549 ± 1 nm, where the Fe²⁺Cc–Fe³⁺Cc difference spectrum is near a maximum (Margoliash & Frohwirt, 1959). Figure 3 shows data for I of the complex [(ZnP)CcP,Cc(horse)] in 10 mM KP_i (pH 7).

As shown before (Wallin *et al.*, 1991), such data is well-described by a sum of three kinetic phases (eq 7). In particular, the trace in Figure 3 is described by the relative weights of $f_1 = 0.78$, $f_2 = 0.11$, and $f_3 = 0.11$ and decay constants for I of $k_1 = 2100$ s^{-1}, $k_2 = 25$ s^{-1}, and $k_3 = 9$ s^{-1}. Phase 1 contributes a rapid absorbance rise that is not well-visualized here; it is shown better for Cc(F:*Ck*) in Figure 6B below. Phases 2 and 3 produce a biexponential fall at rate constants of k_2 and k_3 that is observed after the decay of the triplet state; $t \gg 1/k_{obs}$. As I is formed from ^{3}(ZnP)CcP → Fe³⁺Cc et, the concentration of I reflects the extent of binding in the triplet state. However, in order to quantify the I signal, we must first understand its progress curve. Analysis with eq 7 assumes that only intracomplex et processes are being studied, yet the ^{3}(MgP)CcP decays in the presence of Fe³⁺Cc(horse) in 10 mM KP_i (pH 7) (Figure 2B) showed that $k_{off} > 50$ s^{-1} > k_2, k_3. Thus, one must consider whether the slow decay of the I signal might instead reflect the dissociation of I and a second-order recombination of (ZnP)⁺CcP and Fe²⁺Cc, rather than intramolecular et.

If the progress curve of I at $t \gtrsim 5/k_{obs} \approx 80$ ms in fact reflects second-order processes, then a plot of the inverse absorbance of I versus time should be linear. Figure 3 (inset) clearly shows that such a plot for [(ZnP)⁺CcP,Fe²⁺Cc(horse)] in 10 mM KP_i (pH 7) is not linear, namely, not second-order, for $t \lesssim 300$ ms. Beyond this time, only ≤5% of I remains and the signal is too small for truly definitive statements regarding reaction order. Thus, the assumptions implicit in the use of eq 7 are valid at least for times $t \lesssim 0.3$ s. This result requires that Fe²⁺Cc(horse) dissociates from (ZnP)⁺CcP in 10 mM KP_i (pH 7) with a rate constant of $k_{off} \lesssim k_3 \approx 10$ s^{-1}, which is in marked contrast to the conclusion that $k_{off} \geq 50$ s^{-1} for the complexes of ^{3}(MP)CcP with Fe³⁺Cc(horse), i.e., that $k_{off}(D^+A^-) \ll k_{off}(^3DA)$ (Figure 1).

Equilibrium Constants from Triplet Quenching Titrations. Figure 4A presents quenching titrations of ^{3}(ZnP)CcP by Fe³⁺Cc from horse, *Pichia membranefaciens*, and *Saccharomyces cerevisiae* in 50 mM KP_i (pH 7). This buffer was chosen because ^{3}(MP)CcP decays exponentially for all Cc/CcP ratios and with all cytochromes in this medium, indicating a rapid association equilibrium for Fe³⁺Cc. The figure shows clearly that the several Fe³⁺Cc(F)'s quench ^{3}(ZnP)CcP much more efficiently than does Fe³⁺Cc(horse) over the range of [Cc] studied; a similar division into two evolutionary classes was observed earlier in the responses of ^{3}(ZnP)CcP quenching to temperature and solvent composition (Nocek *et al.*, 1991). The 1:1 binding isotherm of eq 4 adequately represents the data for Cc(horse) (Figure 4A,B) and for the two fungal Cc (solid lines in Figure 4A) in this buffer. A closer inspection of Figure 4A shows that Cc(F:*iso-1*) binds to (ZnP)CcP with somewhat greater affinity than does Cc(F:*Pm*); $^1K_d = 1.4$ μM for the former and 3.2 μM for the latter Cc. The magnitudes of the binding affinities and quenching constants for Cc(F:*Pm*) and Cc(F:*iso-1*) are typical of the values for a variety of fungal Cc in our system and justify our designation of Cc(*Pm*) and Cc(*Ck*) as representative of iso-1 Cc.

Figure 4A also shows k_q for a titration of (ZnP)CcP with Cc(F:*iso-1*) in a buffer of lower concentration (10 mM KP_i, pH 7). The sharp break at a ratio of Cc/CcP ≈ 1 shows that (ZnP)CcP binds Cc(F:*iso-1*) more strongly in this medium, with the estimated value, $^1K_d \leq 0.05$ μM, being in excellent agreement with $K_d = 0.05$ μM reported in a recent study of singlet (MgP)CcP quenching (Corin *et al.*, 1991). However, comparison of this data with a calculated 1:1 isotherm for which $^1K_d = 0.05$ μM and $^1k_Q = 172$ s^{-1} (dotted line in Figure 3A) shows that eq 4 does not rigorously apply to this data because k_q continues to increase slightly as Cc(iso-1) is added well past what would be the saturation point: Cc/CcP ≈ 1. This requires interaction of the 1:1 complex with a second

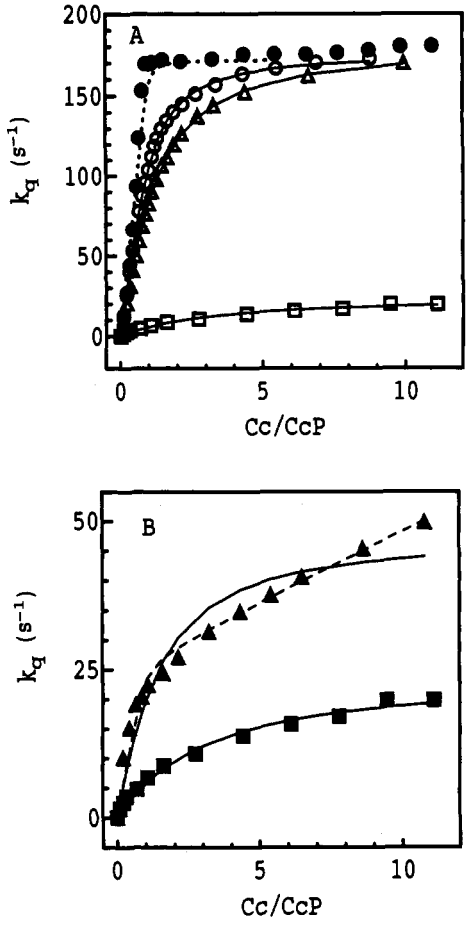

FIGURE 4: Dependence of quenching titrations of ^{3}(ZnP)C*c*P by Fe^{3+}C*c* upon buffer and species of C*c*. (A) Plots of the quenching constant, k_q, versus C*c*/C*c*P for titrations of (ZnP)C*c*P in 50 mM KP_i (pH 7) by C*c*(F:iso-1) (○), C*c*(F:*Pm*) (△) and C*c*(horse) (□). Solid lines are fits to a 1:1 binding isotherm (eq 4, Table I). Also shown is the quenching profile for C*c*(F:iso-1) (●) in 10 mM KP_i (pH 7). The ^{3}(ZnP)C*c*P decays were nonexponential in the range $0 < Cc/CcP < 1$ during this titration. For consistency with the data of higher ratios where curves are exponential, the data in this range are presented as the average quenching values obtained from single-exponential fits, rather than as fractions from eq 6. The dotted line is a simulated 1:1 binding curve for which $^1K_d = 0.05$ μM and $^1k_Q = 172$ s^{-1}. (B) Quenching profiles at pH 7 for Fe^{3+}C*c*(horse) in 10 mM KP_i (▲) and 50 mM KP_i (■). Solid lines again are fits to eq 4; the dashed line is a fit to a 2:1 binding isotherm (eq 5a). Conditions for all titrations: $[(ZnP)CcP]_0 = 5 \pm 0.5$ μM; 20 °C.

molecule of Fe^{3+}C*c*. Indeed, this behavior is strongly accentuated in a titration of (ZnP)C*c*P with Fe^{3+}C*c*(F:*Ck*) in 1 mM KP_i (Figure 5A) and is typical of fungal C*c* in buffers with $[P_i] \leq 10$ mM. Although the increase in k_q when C*c* is added well past the 1:1 point is not always obvious for fungal C*c* (e.g., Figure 4A), it *is* obvious for C*c*(horse) (Figure 4B) and in fact is a general behavior exhibited by *all* cytochromes we have studied.

Figure 4B shows that the profile of k_q for a titration of (ZnP)C*c*P with Fe^{3+}C*c*(horse) in 50 mM KP_i (pH 7) is satisfactorily represented by a 1:1 binding curve (eq 4), with $^1K_d = 12$ μM and $^1k_Q = 24$ s^{-1}. However, when $[P_i]$ is decreased to 10 mM, it is clear that the quenching profile is no longer adequately described by a 1:1 binding curve. Instead, this data can be fit to eq 5a for 2:1 binding. The fit gives $^1K_d = 0.14$ μM and $^1k_Q = 27$ s^{-1} for binding of the first C*c* and $^2K_d \gg [CcP]$ for binding of the second C*c*. This binding to a low-affinity site leads to a nearly linear increase in quenching above $Cc/CcP = 1$. The additional quenching is described

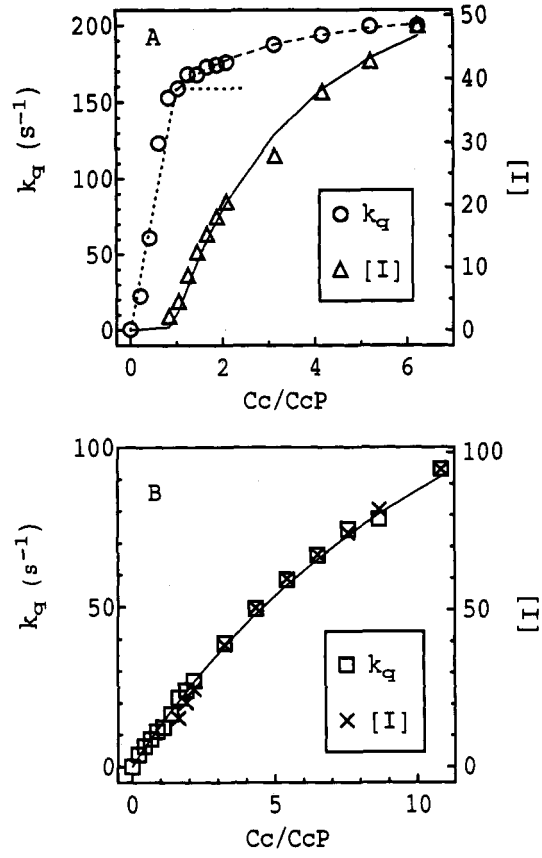

FIGURE 5: Profiles of k_q and [I] during titrations of ^{3}(ZnP)C*c*P with C*c*(horse) and C*c*(F:*Ck*). (A) The triplet quenching rate constant, k_q (○), and the normalized absorbance maximum of the et intermediate, [I] (eq 9) (△), plotted against the molar ratio (C*c*/C*c*P) for a titration of ^{3}(ZnP)C*c*P with Fe^{3+}C*c*(F:*Ck*). The dotted line is a simulated 1:1 binding isotherm (eq 4) for which $^1K_d = 0.001$ μM and $^1k_Q = 159$ s^{-1}. The dashed line is a fit of the quenching profile at $Cc/CcP \geq 1$ to a 2:1 binding isotherm (eq 5a), described by $^2K_d = 10$ μM and $^2k_Q = 60$ s^{-1} when the above site 1 parameters are used. The solid line through the [I] data is a fit to a 2:1 binding isotherm described by $^2K_d = 10$ μM, assuming a high-affinity but et-inactive site 1 with $^1K_d = 0.001$ μM and $^1k_t = 0$ s^{-1}. During this titration with C*c*(F:*Ck*), ^{3}(ZnP)C*c*P decays were biexponential (eq 6) when $0 < Cc/CcP < 1$, as expected when $k_{off} < k_D$; for consistency, plotted numbers for k_q in this range represent average quenching values obtained from fits to a single-exponential decay, as in Figure 4A. (B) Plot of k_q (□) and [I] (×) for a titration of (ZnP)C*c*P with Fe^{3+}C*c*(horse). The solid line is a fit of the k_q profile to eq 4 and is described by $^1K_d = 73$ μM and $^1k_Q = 222$ s^{-1}. Conditions: 20 °C; 1 mM KP_i (pH 7); $[(ZnP)CcP]_0 = 4.4$ and 5.1 μM for parts A and B, respectively.

as

$$\Delta k_q = ({}^2k_Q/{}^2K_d)[Cc] = k_s[Cc] \qquad (10)$$

where Δk_q is the incremental quenching decay constant over that at saturation of the high-affinity site ($k_q \approx 25$ s^{-1} in Figure 4B). The slope for the linear increase in k_q for Fe^{3+}C*c*(horse) binding to (ZnP)C*c*P in 10 mM KP_i (pH 7) is $k_s = {}^2k_Q/{}^2K_d \approx 0.5$ mM^{-1} s^{-1}. An alternative view of this data would be that there is only one well-defined binding site for C*c* on (ZnP)C*c*P and that the linear increase in quenching at high [C*c*] merely reflects additional nonspecific, Stern–Volmer quenching (Turro, 1978) of the 1:1 complex with rate constant k_s. The data shown in Figure 4 does not, by itself, permit a distinction of these two views.

Surprisingly, the titration with Fe^{3+}C*c*(horse) at yet a lower buffer concentration, 1 mM KP_i (pH 7), again is well-described by a 1:1 isotherm, with $^1K_d = 73$ μM and $^1k_Q = 222$ s^{-1} (Figure

5B). This quenching profile exhibits minimal curvature up to Cc/CcP ≈ 10 (Figures 5B and 9B), where $k_q \approx 90\ s^{-1}$, and thus *appears* to reflect weak 1:1 binding of *Cc*(horse) to the peroxidase (*vide infra*). The titration of (ZnP)CcP with Fe^{3+} fungal Cc from *C. krusei* in 1 mM KP_i (pH 7) yields strikingly different results from Cc(horse), as shown in Figure 5A. The quenching rate constant, k_q, rises sharply as Cc/CcP approaches unity and then climbs more gradually with increasing [Cc] above Cc/CcP = 1. The break in the curve indicates strong 1:1 binding of the Fe^{3+}Cc(F:*Ck*) to (ZnP)CcP in this buffer, whereas the quite obvious continuing increase in k_q for Cc/CcP > 1 again must arise from quenching of the 1:1 complex by a second molecule of Cc.

Binding Stoichiometry through Parallel Measurements of k_q and I. The titrations of (ZnP)CcP in buffers with $1 \leq [P_i] \leq 10$ mM with both Cc(horse) and Cc(F) are not fully described in terms of a 1:1 binding stoichiometry, but the quenching data do not definitively characterize the interaction between the 1:1 complex and a second molecule of Cc, an ambiguity typical of quenching measurements. Instead, such a characterization is achieved by *pairing* direct observations of the et intermediate (**I**) with the measurements of quenching of ^{3}(ZnP)CcP by Fe^{3+}Cc. Because **I** is formed by intracomplex ^{3}(ZnP)CcP → Fe^{3+}Cc et, the yield of **I** reflects only the concentration of excited precursor complex that is et-active. Thus, measurements of **I** allow us to assay specifically for et-productive binding to ^{3}(ZnP)CcP, whereas the quenching constant includes all quenching contributions; pairing the two types of measurements allows us to discriminate between productive and nonproductive binding. We accomplish this by correlating values of the quenching constant, k_q, with the quantity [**I**], the maximum absorbance (A_{max}) in the kinetic progress curve for the et intermediate, **I**, normalized relative to the concentration of triplet (eq 9).

Figure 6 shows kinetic progress curves for **I** at several different Cc/CcP ratios during a titration of (ZnP)CcP with Cc(F:*Ck*) in 1 mM KP_i (pH 7). The top panel shows the full time courses of the intermediate, while the bottom panel presents only the early time rises. As expected, the signal clearly grows larger as Cc/CcP increases, with the yield of the intermediate as characterized in terms of [**I**] being plotted in Figure 5A. The shapes of the **I** progress curves do not change appreciably during the titration except to reflect the increase in k_{obs}, consistent with the first-order kinetics of eq 7 and as expected from the analysis of Figure 3. For the relatively small signals early in the titration, there is considerable scatter in the fit parameters. However, for progress curves with $A_{max} \geq 0.001$, the S/N is good enough that the fit parameters are better determined; all such curves in the titration with Cc(F:*Ck*) are well-described by a single global set of parameters: $f_1 \approx 0.75$, $k_1 \approx 3400\ s^{-1}$; $f_2 \approx 0.06$, $k_2 \approx 12\ s^{-1}$; and $f_3 \approx 0.19$, $k_3 \approx 2.5\ s^{-1}$. These parameters are in good agreement with those recently published for Cc(F:*Ck*) in this buffer (Wallin *et al.*, 1991). Indeed, for all Cc in buffers with $1 \leq [P_i]\ 1 \leq 10$ mM, the fit parameters are invariant with changes in Cc/CcP, confirming our earlier finding that the progress curves for **I** are not influenced by bimolecular processes under these low ionic strength conditions (Figure 3). As μ is increased further, k_{off} for Fe^{2+}Cc also will increase, and at some point it is likely that dissociation will become fast enough to occur during the lifetime of the transient. Data presented in Figure 7 suggest that dissociation is not significant for $\mu \lesssim 50$ mM; future work will explore this question more fully.

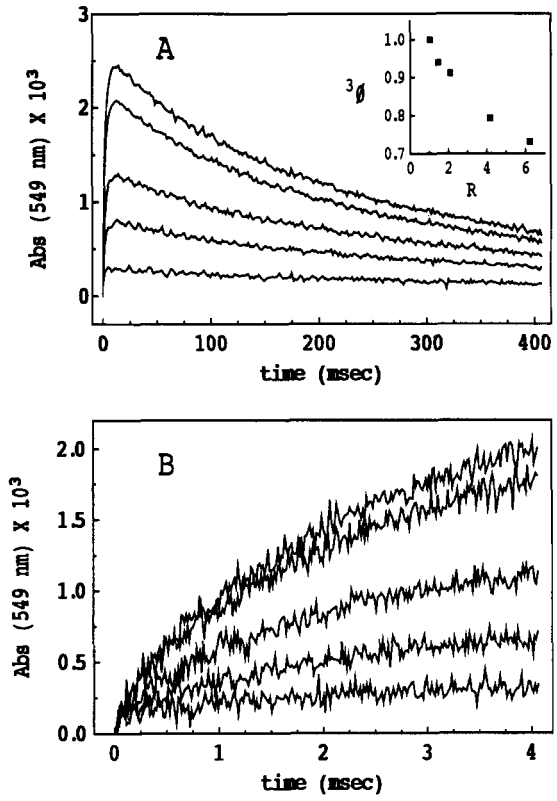

FIGURE 6: Growth of signal for electron-transfer intermediate **I** during a titration of (ZnP)CcP with Fe^{3+}Cc(F:*Ck*). Kinetic progress curves of **I** at 549 nm are shown for *R* (= Cc/CcP) values of 1.0, 1.5, 2.1, 4.2, and 6.2. Both the appearance (B) and full time course (A) of **I** are shown. Inset: A plot of the corresponding values of the triplet yield ($^3\phi$) obtained by dividing the zero-time ^{3}(ZnP)CcP absorbance change (475 nm) by the value at $R = 1.0$ ($\Delta A(t{=}0,475\text{nm}) = 0.0702$). Conditions: $[(ZnP)CcP]_0 = 4.4\ \mu M$; 1 mM KP_i (pH 7); 20 °C.

The results of the joint measurements of quenching and the et intermediate for titration of (ZnP)CcP with Fe^{3+}Cc(F:*Ck*) in 1 mM KP_i (pH 7) are presented in Figures 5 and 6. The most striking feature of the titration is the *lack* of correlation between the increases in k_q and the amount of et intermediate formed: the appearance of **I** lags well behind the increase in quenching as Fe^{3+}Cc(F:*Ck*) is added to (ZnP)CcP. As seen in Figure 6, **I** is barely visible at a 1:1 ratio of the two proteins, where $k_q \approx 160\ s^{-1}$; the raw signal for **I** then grows sharply as Cc is added past the 1:1 point, whereas k_q increases minimally. Indeed, this dramatic *increase* in the signal height for **I** occurs despite the fact that the triplet yield actually *decreases* (Figure 6, inset) with increasing Cc/CcP, for reasons noted above. Normalization of the maximum absorbance of **I** relative to the triplet concentration accentuates the lag. The yield of et intermediate, [**I**], increases by a factor of ~15 as the Cc/CcP ratio is increased from Cc/CcP = 1.0 to 6.2, whereas k_q increases by only 25% (from 160 to 200 s^{-1}) in this range.

The quenching titration curve of Figure 5 clearly implies that the majority of observed ^{3}(ZnP)CcP quenching by Fe^{3+}Cc(F:*Ck*) is associated with tight 1:1 binding, as expected at such a low ionic strength (Corin *et al.*, 1991; Vitello & Erman, 1987). However, the growth of the signal for **I** upon the addition of Cc well past the point where the quenching curve shows a "break" rules out a simple 1:1 binding interaction, since the strongly binding and strongly quenching site of the peroxidase should already be nearly saturated with cytochrome at an equimolar ratio of the proteins. This behavior in fact is general for Cc(F): the appearance of **I** also lags k_q in titrations with the *P. membranefaciens* and iso-1 cytochromes

at low ionic strength. The simplest interpretation for the lack of correlation between k_q and [I] for *Cc*(F) is that (ZnP)*Cc*P successively binds two molecules of Fe^{3+}*Cc*(F): the first *Cc* molecule binds tightly at site 1 and quenches primarily by a nonredox mechanism, while the second molecule binds more weakly at a second site (site 2) that nonetheless exhibits relatively efficient quenching by et.[7]

The lag in [I] during the titration of (ZnP)*Cc*P with *Cc*(F:*Ck*) in 1 mM KP_i (pH 7) can be reproduced with a 2:1 binding isotherm (eq 5a). Consider as a *limiting* case that (ZnP)*Cc*P first strongly binds an Fe^{3+}*Cc*(F:*Ck*) ($^1K_d < 0.05$ μM) at a site that is quenched efficiently ($^1k_Q = 159$ s^{-1}) but is redox-inactive ($^1k_t = 0$ s^{-1}), and that it also weakly binds a second *Cc* molecule at a site (site 2) where quenching occurs only by electron transfer ($^2k_Q = {}^2k_t$). With these constraints, a fit of the observed binding profile of [I] to eq 5a yields a binding constant for the second *Cc* of $^2K_d = 11$ μM (Figure 5A). An independent application of the model to the triplet quenching profile at *Cc*/*Cc*P > 1 gives good agreement with experiment (Figure 5A), with $^2K_d = 10$ μM and $^2k_Q = 60$ s^{-1}. The close agreement between the ^2K_d values obtained by the two fits clearly links the increase in k_q at *Cc*/*Cc*P > 1 to formation of the electron-transfer intermediate. Similar parallel measurements with *Cc*(F:iso-1) and *Cc*(F:*Pm*) cytochromes show the same lag in [I] relative to k_q during titrations. Thus, all of the fungal *Cc* studied show 2:1 complex formation: the first Fe^{3+}*Cc*(F) binds to a high-affinity site that is strongly quenched yet is et-inactive, and the second Fe^{3+}*Cc*(F) binds to a low-affinity site that allows efficient electron transfer quenching.

Equivalent experiments show that *Cc*(horse) behaves quite differently from *Cc*(F). Figure 5B shows that k_q and [I] increase in synchrony during a titration of (ZnP)*Cc*P with Fe^{3+}*Cc*(horse) in 1 mM KP_i (pH 7). This synchrony requires that nearly all (or a constant percentage at all *Cc*/*Cc*P) of the quenching by Fe^{3+}*Cc*(horse) occur by an electron-transfer mechanism, and it is *consistent* with (*vide infra*) weak 1:1 binding of *Cc*(horse) to (ZnP)*Cc*P. This observation of a correlation between k_q and [I] for *Cc*(horse) in 1 mM KP_i (pH 7) further lends credence to the lack of correlation seen with *Cc*(F:*Ck*).

Dissociation of [(ZnP)CcP,Fe³⁺Cc] with KCl. To complement the above measurements, we titrated complexes of (ZnP)*Cc*P with both *Cc*(horse) and *Cc*(F) with KCl to raise the ionic strength to look for the relationship between the loss of quenching and the loss of the I signal as the complexes progressively dissociated.

Consider an experiment that begins with the complex of (ZnP)*Cc*P and *Cc*(horse) at a 1:11 ratio and in a low ionic strength buffer that maximizes electrostatic binding, 1 mM KP_i (pH 7). Progressive additions of KCl to the sample dissociate the complex, as shown by the increasing triplet lifetimes (Figure 7, inset) and decreasing quenching constants (Figure 8A). At the highest concentration of added salt ([KCl] = 213 mM), the binding of *Cc*(horse) to the peroxidase is nearly abolished, as indicated by the nearly complete loss of quenching (Figure 8A).

The parallel effects of added KCl on the progress curves for the et intermediate, [$(ZnP)^+$*Cc*P,Fe^{2+}*Cc*(horse)], are

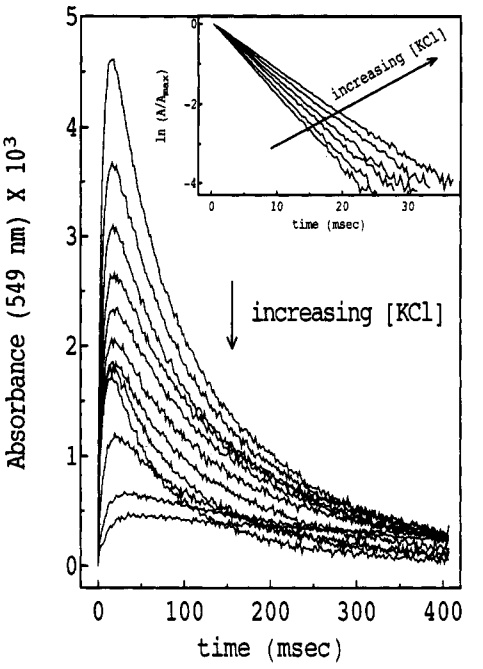

FIGURE 7: Effect of added KCl upon kinetic progress curves at 549 nm for I formed upon flash photolysis of (ZnP)*Cc*P in the presence of excess Fe^{3+}*Cc*(horse). Shown in descending order of signal height is I at [KCl] = 0, 2.6, 5.2, 7.7, 10, 15, 20, 31, 49, 100, 156, and 213 mM. Inset: A semilog plot of triplet decay traces for [KCl] = 0, 2.6, 10, 49, 100, and 213 mM. Conditions: $[(ZnP)CcP]_{total} = 5.2$ μM before addition of KCl; *Cc*/*Cc*P ≈ 11; 1 mM KP_i (pH 7); 20 °C; KCl stock solutions also contained 1 mM KP_i buffered at pH 7 so that pH and $[P_i]$ would be constant during the experiment.

shown in Figure 7; corresponding values of the normalized absorbance maximum, [I], are plotted in Figure 8A. Over most of the experiment, the major effect of adding KCl is to decrease the amount of I formed. As [KCl] increases from 0 to 50 mM, the shapes of the progress curves for I (Figure 7) remain essentially unchanged, except to reflect the decrease in the triplet decay rate constant, k_{obs}, and only at the highest salt concentrations ([KCl] ≥ 100 mM) does the long time decay of I clearly slow. Comparison of the results for the two probes (Figure 8A) shows that, as the [(ZnP)*Cc*P,*Cc*(horse)] complex is dissociated by KCl, k_q and [I] decrease smoothly and synchronously: at a given salt concentration, the fractional decrease in k_q correlates well with the fractional decrease in [I]. Again the joint measurements indicate that the quenching by this ferricytochrome *c* is predominantly electron transfer, i.e., $k_q \approx k_t$, as expected from Figure 5B.

The behavior of the complex with *Cc*(F:*Pm*) contrasts sharply with that involving *Cc*(horse): k_q and [I] for *Cc*(F:*Pm*) do *not* change synchronously upon the addition of KCl (Figure 8B). The ^{3}(ZnP)*Cc*P quenching is clearly lost in two major steps. The value of k_q drops from 220 to 175 s^{-1} as [KCl] increases from 0 to 50 mM, changes little up to [KCl] = 100 mM, and then drops sharply to a value of ~40 s^{-1} as [KCl] increases further to 213 mM. The ^{3}(ZnP)*Cc*P → Fe^{3+}*Cc* electron-transfer process behaves quite differently. Additions of KCl up to [KCl] = 50 mM mostly eliminate this reaction, as evidenced by the sharp decrease in [I], with further increases in [KCl] having little effect. In short, the ^{3}(ZnP)*Cc*P → Fe^{3+}*Cc*(F:*Pm*) electron-transfer component of the ^{3}(ZnP)*Cc*P quenching is largely abolished at an ionic strength where ~75% of the initial quenching is retained. These results imply that the low-affinity site, at which most of the photoinitiated reduction of Fe^{3+}*Cc*(F) occurs, is quite sensitive to ionic strength and that the high-affinity site, at which most of the quenching occurs by a nonredox mechanism, is less

[7] We recognize, but henceforth ignore, the inverse possibility that the k_b for intermediate formed at site 1 is so large (≳10^5 s^{-1}) that by eq 7 the associated absorbance change is not detectable. Firstly, for purposes of establishing stoichiometry, this issue is immaterial. Secondly, although we at present prefer the view presented in the text, the issue is by no means settled definitively and merits further experiments.

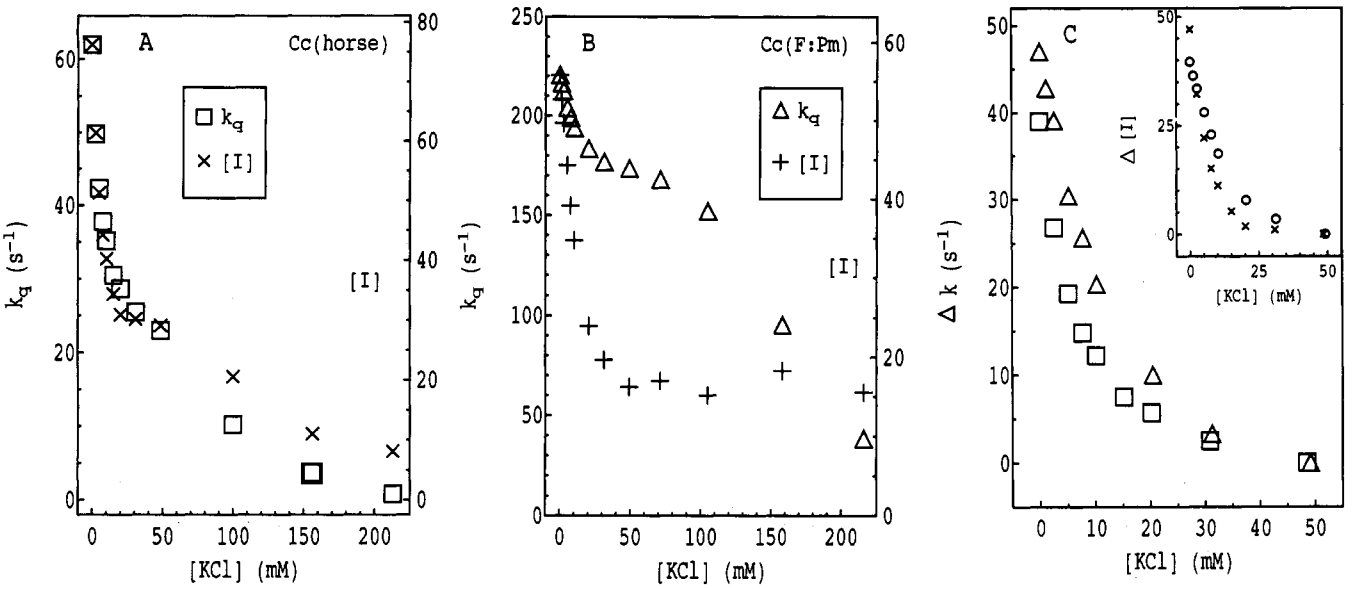

FIGURE 8: Responses of k_q and [I] to additions of KCl to (ZnP)CcP in the presence of excess (A) Fe^{3+}Cc(horse) and (B) Fe^{3+}Cc(F:*Pm*). (A) The values of k_q (□) and [I] (×) for [(ZnP)CcP,Cc(horse)] as [KCl] is increased to 213 mM. (B) The values of k_q (Δ) and [I] (+) as [KCl] increases from 0 to 216 mM for (ZnP)CcP in the presence of Cc(F:*Pm*). (C) Changes of k_q and [I] in the range 0–50 mM KCl for complexes of (ZnP)CcP with Cc(horse) (□) and Cc(F:*Pm*) (Δ). Values of Δk were calculated from data in A and B as $\Delta k = k_q([KCl]) - k_q([KCl] = 50\ mM)$; values of Δ[I] were obtained in a similar manner. Inset: Plot of Δ[I] versus [KCl] for Cc(horse) (×) and Cc(F:*Pm*) (○). Conditions: $[(ZnP)CcP]_{total} = 5.1 \pm 0.1\ \mu M$ before addition of KCl; Cc/CcP ≈ 11; 1 mM KP_i (pH 7). Addition of buffered KCl stock solutions resulted in a dilution of the samples by ~15% by the end of the experiments.

Table I: Binding Constants for Fe^{3+}Cc

Cc	$[P_i]$ (mM)	pH	^1K_d (μM)	^1k_Q (s^{-1})	k_s ($\mu M^{-1}\ s^{-1}$)	$^1k_{off}$ (s^{-1})	$^2k_{off}$ (s^{-1})	footnote
fungal								
P. membranefaciens	1	7	≤0.05	175	0.57	<120		*a*
	10	7	≤0.05	175	0.30	<200[b]	≥10^4 [c]	*a*
	50	7	3.2	181		>300		*d*
	50	7	2.8	171		>300		*d, e*
C. krusei	1	7	≤0.05	168		<120		*a, f*
	10	6	≤0.05	175	0.27	<200[b]	≥10^4 [c]	*a*
	10	7	≤0.05	176	0.38	<200[b]		*a*
	10	8	≤0.05	172	0.45	<200[b]		*a*
iso-1	10	7	≤0.05	172	0.21	<200[b]	≥10^4 [c]	*a*
	50	7	1.4	177		>300		*d*
vertebrate								
horse	1	7						*d, g*
	5	7	0.06	22	0.80			*h*
	10	7	0.15	26	0.51			*h*
	50	7	12	24		(>50)	≥10^4 [c]	*d*
	10	6	0.63	24	0.17			*h*
	10	8	0.06	37	0.76			*h*
tuna	10	7	0.06	26	0.20	>50	≥10^4 [c]	*h*

[a] ^{3}(MP)CcP decays were nonexponential when $0 < Cc/CcP < 1$ for this combination of fungal cytochrome *c* and low ionic strength buffer, setting an upper limit on $^1k_{off}$. Upper limits on ^1K_d were obtained from fits of the fraction bound (to site 1 of (ZnP)CcP) to eq 6, used for 1:1 binding in the slow-exchange limit. In these cases, values of ^1k_Q do not represent the fit results of eq 4, but rather are the measured values of k_q at $Cc/CcP = 1.3 \pm 0.3$. The value of k_s ($= {}^2k_Q/{}^2K_d$), which defines the weak binding interaction of the second Fe^{3+}Cc, was estimated from the slope of the quenching profile at $Cc/CcP \geq 1.3$, where ^{3}(MP)CcP decays were exponential. [b] A lower limit of $^1k_{off} > 20\ s^{-1}$ was also found. [c] Assuming $^2K_d \geq 100\ \mu M$ and $^2k_{on} = 10^8\ s^{-1}$. [d] ^{3}(MP)CcP decays were exponential for all Cc/CcP for this combination of cytochrome *c* and buffer. The quenching profile was described well by a 1:1 binding isotherm (eq 4), and these values of ^1K_d and ^1k_Q have uncertainties of ±25% and ±10%, respectively. [e] These values of ^1K_d and ^1k_Q are from a titration of (MgP)CcP. [f] A fit of this Fe^{3+}Cc(F:*Ck*) quenching profile at $Cc/CcP > 1$ gave $^2K_d = 10\ \mu M$ and $^2k_Q = 60\ s^{-1}$. [g] A fit to eq 4 adequately describes this quenching profile, with $^1K_d = 73\ \mu M$ and $^1k_Q = 222\ s^{-1}$. However, 1:1 binding is not expected in this buffer (see text), and the fit results probably reflect the weak binding of a second molecule of Fe^{2+}Cc(horse) to form the 2:1 complex. Thus, we omit the fit results from the table. [h] ^{3}(MP)CcP decays were exponential for all Cc/CcP for this combination of cytochrome *c* and buffer. The quenching profile was not adequately described by a 1:1 binding isotherm (eq 4). The data was instead fit with a 2:1 binding isotherm (eq 5a). Values of ^1K_d, ^1k_Q, and k_s have uncertainties of ±100%, ±10%, and ±5%, respectively.

sensitive to ionic strength. As in the titration of (ZnP)CcP with Fe^{3+}Cc(F:*Ck*) (Figure 5), the detection of two modes of quenching (and 2:1 binding) is possible only through the joint measurements of k_q and [I]. The constant, small value of [I] at high ionic strength may indicate bimolecular ^{3}(ZnP)CcP → Fe^{3+}Cc electron transfer; such a change in mechanism might be expected from the change in shape of the progress curve of I for Cc(horse) when [KCl] ≥ 100 mM.

The relative affinities of Cc(F) and Cc(horse) for sites 1 *and* 2 of (ZnP)CcP are accessible from a closer look at the data of Figure 8. Consider first site 2. Table I shows that at pH 7, $^1k_Q \approx 175$ and 25 s^{-1} for Fe^{3+}Cc(F:*Pm*) and Fe^{3+}Cc(horse), respectively. For [KCl] ≲ 50 mM, the observed quenching constant, k_q, is greater than the intramo-

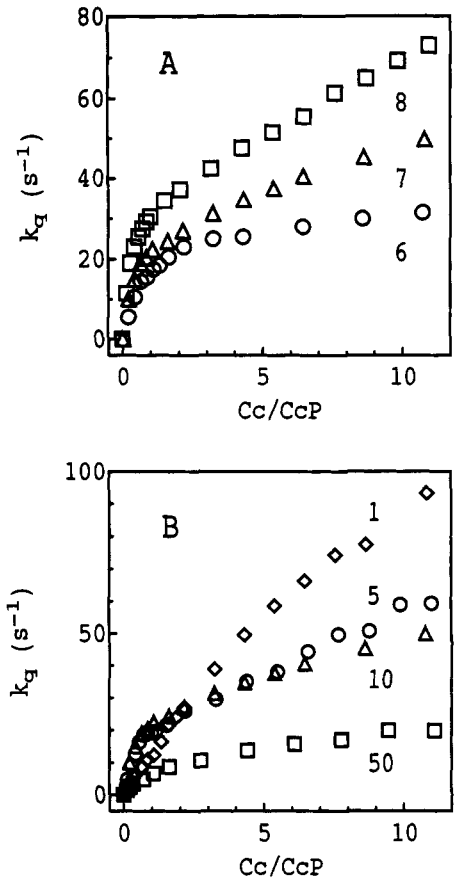

FIGURE 9: Effect of pH (A) and [P_i] (B) upon quenching titrations of (ZnP)CcP with Fe^{3+}Cc(horse). (A) Plots of k_q versus Cc/CcP for titrations in 10 mM KP_i buffered at pH 6 (○), pH 7 (△), and pH 8 (□). (B) Plots of k_q versus Cc/CcP at pH 7 for [P_i] = 1 (◇), 5 (○), 10 (△), and 50 (□). Conditions: [(ZnP)CcP]$_0$ = 5 ± 0.5 μM; 20 °C.

lecular quenching constant for the 1:1 complex with site 1 fully bound with Fe^{3+}Cc, and the difference $k_q - {}^1k_Q$ represents the quenching due to Fe^{3+}Cc bound at site 2. Therefore, for each value of [KCl] < 50 mM, the difference $\Delta k = k_q - k_q$(50 mM KCl) $\approx k_q - {}^1k_Q$; a quantity, Δ[I], for the yield of et intermediate at site 2 is defined in an analogous manner. Figure 8C shows that plots of Δk and Δ[I] behave very similarly for the two Cc in the range 0–50 mM KCl, where Cc is dissociated only from site 2 of (ZnP)CcP and site 1 remains occupied. This suggests that the two cytochromes have similar affinities for site 2, with the slightly sharper response to salt seen for Cc(horse) perhaps indicating a modest preference for Cc(F) at site 2.

Figure 8 confirms that the affinity of site 1 under much higher ionic strength conditions is higher for Fe^{3+}Cc(F) than for Fe^{3+}Cc(horse), as expected from the titration data in 50 mM KP_i (pH 7) (Figure 4, Table I). At [KCl] ≈ 210 mM, where only the 1:1 complex would be observed, $k_q \approx 1\ s^{-1}$ for Cc(horse) and 40 s^{-1} for Cc(F:*Pm*). The ratio $k_q/{}^1k_Q$, i.e., the fraction bound at site 1, is smaller for Cc(horse) than for Cc(F:*Pm*), consistent with our titrations in 50 mM KP_i (pH 7) (Figure 4) and with other studies (Leonard & Yonetani, 1974; Kang *et al.*, 1977; Vitello & Erman, 1987) which show that the binding and kinetics of Cc(horse) are more sensitive to ionic strength than are those for Cc(F).

Effect of pH and Ionic Strength upon Binding of Cc(horse). Figure 9 illustrates how changes in pH and [P_i] influence the binding of Fe^{3+}Cc(horse) by (ZnP)CcP. Figure 9A shows that the quenching increases with pH for titrations of ZnCcP in 10 mM KP_i and that the character of the titration curves changes as well. At pH 6, the data can be nearly described with a 1:1 binding isotherm (eq 4), whereas at higher pH, the profiles become increasingly nonhyperbolic and no longer allow a simple description in terms of binding a single molecule of Fe^{3+}Cc(horse) to (ZnP)CcP. Figure 9A suggests that the apparent simplicity of much of the data for Cc(horse) disguises a closer parallel with Cc(F), namely, that (ZnP)CcP can also bind two molecules of Cc(horse). Fits to eq 5a, which assume 2:1 binding, suggest that the affinity of Cc(horse) for site 1 may increase with pH (Table I), despite the fact that the ionic strength of 10 mM KP_i also increases with pH. However, as the 2:1 fits give ${}^1K_d \ll$ [CcP], this is not particularly conclusive, and Vitello and Erman (1987) found little change in K_d for Cc(horse) between pH 6 and 7.5.

In any case, the differences in the appearance of the curves at different pH values arise primarily from an increase in the quenching rate constants for site 1 (${}^1k_Q$) and in the "bimolecular" quenching constant for site 2 ($k_s = {}^2k_Q/{}^2K_d$) (Table I). The intramolecular quenching rate constant for site 1 increases somewhat, from ${}^1k_Q = 24\ s^{-1}$ at pH 6 to ${}^1k_Q = 38\ s^{-1}$ at pH 8, whereas between pH 6 and 8, the constant, k_s, for site 2 of (ZnP)CcP increases 4-fold from $k_s = 0.18$ to 0.77 $\mu M^{-1}\ s^{-1}$. The trend in k_s appears to hold for Fe^{3+}Cc(F:*Ck*) as well (Table I). The increase in k_s with pH could be attributed to either an increase in ${}^2k_Q$ or a decrease in ${}^2K_d$. The latter possibility of tighter binding seems likely, because the Cc–Cc electrostatic repulsion in a 2:1 complex should be lessened with increasing pH.

If we focus on pH 7 (Figure 9B), the data at high Cc/CcP ratios show that k_q increases as [KP_i] decreases, following the expected trend toward increased electrostatic interactions between the two proteins at low μ. An increase in phosphate concentration also changes the binding stoichiometry from 2:1 to 1:1, an effect shown best in Figure 4B. Thus, the binding profile for Fe^{3+}Cc(horse) in 50 mM KP_i appears hyperbolic and can be adequately represented by eq 4, consistent with 1:1 binding to site 1 at this μ, as expected from Figure 8. In contrast, the data for 10 and 5 mM KP_i are obviously nonhyperbolic and thus indicative of 2:1 binding. As seen in Table I, an increase in [P_i] from 5 to 50 mM lowers the affinity of site 1 for Fe^{3+}Cc(horse) by about 100-fold, from ${}^1K_d \approx 0.1$ μM (5 mM KP_i) to ${}^1K_d \approx 12$ μM (50 mM KP_i), whereas the quenching constant for site 1 remains roughly constant at ${}^1k_Q \approx 25\ s^{-1}$.

Surprisingly, the k_q binding profile for Fe^{3+}Cc(horse) at yet lower μ, in 1 mM KP_i (pH 7), is indistinguishable from a 1:1 binding isotherm (eq 4) with weak binding (Figures 5B and 9B). However, the ${}^1K_d$ values obtained from one-site fits (eq 4) appear to increase by a factor of ~6 upon lowering the [P_i] from 50 to 1 mM at pH 7 (Table I), which clearly is unreasonable for an electrostatic complex; moreover, the literature suggests that, at this very low ionic strength, Fe^{3+}Cc(horse) should bind very tightly to CcP ($K_d \leq 0.4$ μM) (Vitello & Erman, 1987). Therefore, given that the isotherms of Figure 9B indicate a 2:1 stoichiometry for Cc(horse) in 5 and 10 mM KP_i and that Cc(F)'s bind 2:1 in 1 mM KP_i, it is more economical to assume that Cc(horse) also binds with a 2:1 stoichiometry in 1 mM KP_i. In fact, a 2:1 stoichiometry can lead to a binding profile that is not distinguishable from weak 1:1 binding in cases where site 1 binds tightly, ${}^1K_d \ll$ [CcP] $\ll {}^2K_d$, but quenches poorly, ${}^1k_Q \ll {}^2k_Q$. For example, we can accurately describe the horse titration in 1 mM KP_i with eq 5a. If we constrain ${}^1K_d$ at 0.1 μM, the result is that the affinity for site 2 is ~700-fold lower (${}^2K_d = 67$ μM) but

the quenching constant for site 2 is *ca.* 15-fold greater, with ^2k_Q = 191 s^{-1} while ^1k_Q = 13 s^{-1}.

Fe^{3+}Cc Binding Constants. The results of the quenching titrations are summarized in Table I. In low ionic strength buffers ([P_i] ≤ 10 mM), both Fe^{3+}C*c*(horse) and Fe^{3+}C*c*(F) bind avidly to site 1 of the peroxidase: ^1K_d < 1 μM. Even the apparent exception, Fe^{3+}C*c*(horse) in 1 mM KP_i (pH 7), was shown to be consistent with these conclusions. Because the binding is so tight under these conditions ($^1K_d \ll$ [C*c*P]), it is difficult to determine the relative affinities of the two types of cytochromes. Hence, to examine this question, we consider the data for 50 mM KP_i (pH 7), where the binding is significantly weaker than at low μ. As the second site is largely dissociated at μ = 50 mM (Figure 8), the quenching data in 50 mM KP_i (pH 7) only give information about 1:1 binding at site 1. The data in Table I show that the several fungal C*c* all form stronger 1:1 complexes with (ZnP)C*c*P than does C*c*(horse); for example, ^1K_d = 12, 3.2, and 1.4 μM for the ferric forms of C*c*(horse), C*c*(F:*Pm*), and C*c*(F:iso-1), respectively.

To compare the data with literature values, it is necessary to keep in mind the possibility of specific ion effects, namely, that phosphate binds to cytochrome *c* and could lessen its affinity for C*c*P (Pettigrew & Moore, 1987). We thus limit the comparisons to other studies that used phosphate-containing buffers of similar ionic strength. If we consider first Fe^{3+}C*c*(F:iso-1) at high μ, the binding constants for site 1 agree quite well with literature values. For example, the value of ^1K_d = 1.4 μM for this C*c* in 50 mM KP_i (pH 7) (μ ≈ 100 mM) is similar to K_d = 2.0 μM in pH 7.5 KP_i/KNO_3 buffer (μ = 100 mM) (Erman *et al.*, 1991). These values are also consistent with the value of K_d = 14 μM for the binding of Fe^{3+}C*c*(F:iso-1) to luminescent C*c*P derivatives in 0.1 M KP_i (pH 7) (Leonard & Yonetani, 1974), as well as the strong binding (K_d = 2 μM) of Fe^{3+}C*c*(F:iso-2) to the high-affinity site of Fe^{3+}C*c*P in 0.1 M Tris–P_i (pH 6) (Kang *et al.*, 1977). The binding constants for C*c*(F:*Ck*) and C*c*(F:*Pm*) are the first to be reported, but the strong binding and similar quenching constants confirm that they behave quite similarly to C*c*(F:iso-1). The binding of Fe^{3+}C*c*(horse) has been studied extensively by Vitello and Erman (1980, 1987), and at high ionic strength, they find K_d = 44 μM in pH 7.5 KP_i/KNO_3 buffer (μ = 100 mM), which is somewhat larger than our value of ^1K_d = 12 μM in 50 mM KP_i (pH 7) (μ ≈ 90 mM).

For conditions of low ionic strength, our finding of 2:1 binding stoichiometry is in excellent agreement with the studies of Kang *et al.* (1977). Using the gel-filtration method of Hummel and Dreyer (1962), they found ^1K_d = 0.5 μM for binding of Fe^{3+}C*c*(horse) to the high-affinity site of Fe^{3+}C*c*P in 20 mM Tris–P_i (pH 6) (μ ≈ 20 mM), which is similar to ^1K_d = 0.15 μM for binding of Fe^{3+}C*c*(horse) to (ZnP)C*c*P in 10 mM KP_i (pH 7) (μ ≈ 18 mM). Kang *et al.* (1977) also found that ^2K_d = 20 μM for the low-affinity site, which is noticeably lower than our limit of ^2K_d > 100 μM for the binding of a second C*c* to the 1:1 complex. We cannot compare our low μ results with the thorough investigations of Vitello and Erman (1987) because they analyzed their data in terms of 1:1 binding, and thus their ^1K_d values for Fe^{3+}C*c*(horse) are necessarily larger than those obtained from the 2:1 fits of (ZnP)C*c*P titrations.

Association Rate Constant (k_{on}) at Site 1. The binding constants and bounds on the dissociation rate constants for Fe^{3+}C*c* (Table I) set limits on the magnitude of the association rate constant (k_{on}) for Fe^{3+}C*c* and (MP)C*c*P. We adopt a nomenclature similar to that in Scheme II, where left superscripts of k_{off} or k_{on} refer to the site, and the oxidation state of the cytochrome follows parenthetically. During titrations with C*c*(F:*Pm*) and C*c*(F:iso-1) in 50 mM KP_i (pH 7) (Figure 4A), where only 1:1 binding at site 1 is expected, the decays of ^{3}(ZnP)C*c*P (data not shown) are exponential, indicating that $^1k_{off}(3+) > k_{obs} > 300\ s^{-1}$ for both C*c*'s, which have equilibrium dissociation constants of ^1K_d = 3.2 and 1.4 μM, respectively. The lower limit of $^1k_{off}(3+)$ (300 s^{-1}) corresponds to the lower limits of $^1k_{on}(3+)$ (≥9.3 × 10^7 and 2.1 × 10^8 M^{-1} s^{-1}, respectively). For Fe^{3+}C*c*(horse) in this same buffer, ^1K_d = 12 μM and, correspondingly, $^1k_{on}(3+) \geq 4 \times 10^6$ M^{-1} s^{-1}; the use of k_{off} = 1100 s^{-1} from Satterlee *et al.* (1987) raises this value to 10^8 M^{-1} s^{-1}. In addition, for C*c*(F) in buffers where 1 ≤ [P_i] ≤ 10 mM, $^1K_d \leq 0.05$ μM while $20 < {}^1k_{off}(3+) < 200\ s^{-1}$. Estimating $^1k_{off}(3+)$ and ^1K_d to be 100 s^{-1} and 0.05 μM, we calculate $^1k_{on}(3+) \approx 2 \times 10^9$ M^{-1} s^{-1} for C*c*(F) at low μ, which approaches the diffusion-controlled limit (Berg & von Hippel, 1985). All of these values for the association rate constant at site 1 agree well with the lower limits of 10^8 and 5 × 10^8 M^{-1} s^{-1} reported for C*c*(horse) at 20 mM and zero ionic strength, respectively (Kim *et al.*, 1990).

DISCUSSION

For more than 2 decades, it has been known that cytochrome *c* peroxidase and cytochrome *c* form a complex at low ionic strength (Mochan, 1970). During that time, however, the stoichiometry of binding has been a matter of some dispute, with the general consensus favoring formation of only a 1:1 complex (Mochan & Nicholls, 1971; Gupta & Yonetani, 1973; Leonard & Yonetani, 1974; Erman & Vitello, 1980; Vitello & Erman, 1987; Corin *et al.*, 1991; Moench *et al.*, 1992). However, the present study clearly shows that the peroxidase binds two molecules of Fe^{3+}C*c* at low ionic strength, one with high affinity (site 1, K_d < 1 μM) and one with low affinity (site 2, K_d > 10 μM), confirming the earlier results of Kang *et al.* (1977). Furthermore, for both C*c*(horse) and C*c*(F), the efficiency of ^{3}(ZnP)C*c*P → Fe^{3+}C*c* electron transfer is far greater at the low-affinity site on (ZnP)C*c*P than at the high-affinity site.

The basis for these conclusions regarding C*c*(F) is as follows. In titrations of (ZnP)C*c*P with Fe^{3+}C*c*(F) at low ionic strength, the quenching constant, k_q, rises sharply as Fe^{3+}C*c*(F) progressively binds to site 1, but continues to increase past the point where C*c*P should be saturated with C*c* if binding were 1:1 and only at the high-affinity site. This requires an interaction with a second molecule of C*c*, either by 2:1 complex formation or Stern–Volmer quenching of the 1:1 complex. This inference is confirmed by the observation that the formation of the electron-transfer intermediate, I, lags k_q in titrations of (ZnP)C*c*P at low ionic strength. When C*c*(F) is added past the 1:1 point, where the high-affinity site should be saturated, the yield of ^{3}(ZnP)C*c*P → Fe^{3+}C*c*(F) et, as measured by the normalized signal for the et intermediate, [I], increases dramatically despite only modest increases in k_q (Figure 4A). This clearly shows that et occurs predominantly when the 1:1 complex interacts with a second cytochrome. The fact that Fe^{2+}C*c* dissociates slowly from $(ZnP)^+$C*c*P further indicates that the encounter of the second Fe^{3+}C*c* with the 1:1 complex involves a specific binding interaction.

These data, most specifically the lag in the appearance of I, require that the 1:1 complex of (ZnP)C*c*P with Fe^{3+}C*c*(F) be essentially et-inactive, even though ^{3}(ZnP)C*c*P is strongly quenched, and that electron transfer proceed primarily in the

Table II: Interactions of Fe^{3+}Cc with the Two Sites of (ZnP)CcP[a]

		site 1	site 2
Fe^{3+}Cc(fungal)			
k_{off} (s^{-1})	high μ	>200	$>10^4$
	low μ	<200	$>10^4$
K_d (μM)	high μ	≥1	weak
	low μ	≤0.05	≥100
quenching mode		non-et	et
Fe^{3+}Cc(horse)			
k_{off} (s^{-1})		>50	$>10^4$
K_d (μM)	high μ	≥10	weak
	low μ	<1	≥100
quenching mode		et	et

[a] Sites 1 and 2 are the high-affinity and low-affinity sites, respectively. The fungal Cc's studied here include yeast iso-1, *P. membranefaciens*, and *C. krusei*. Low μ buffer denotes ($1 \leq [P_i] \leq 10$ mM) ≙ ($1.8 \leq \mu \leq 18$ mM); high μ characteristics apply both to buffers with [KCl] ≥ 50 mM and $[P_i] \geq 50$ mM. Quenching mode implies the dominant mode.

2:1 complex. The most straightforward interpretation for this data is that the lag for Cc(F) occurs because of differential reactivity of the two sites on (ZnP)CcP, specifically, that $^1k_t \ll {}^1k_Q \approx 170\ s^{-1}$ while $^2k_Q \approx {}^2k_t \gg {}^1k_t$ (see eq 5a). However, for completeness, one should note that the possibilities (i) of an allosteric effect, where binding of the second Cc in a 2:1 complex serves to make et more efficient at site 1, and (ii) of electron self-exchange occurring between the two Cc bound in the intermediate (Dixon *et al.*, 1989) have not been ruled out.

The arguments for (ZnP)CcP binding two molecules of Fe^{3+}Cc(horse) are similar. The k_q binding profile in 10 mM KP_i (pH 7) clearly does not fit to a 1:1 binding isotherm (Figure 4B), again requiring that the 1:1 complex interact with a second molecule of Fe^{3+}Cc(horse). This nonhyperbolic binding behavior is general for Fe^{3+}Cc(horse) in buffers where $1 \leq [P_i] \leq 10$ mM and is especially obvious at pH 8 (Figure 9A). As with Cc(F), the increases in quenching of ^{3}(ZnP)CcP by Fe^{3+}Cc(horse) at Cc/CcP > 1 are matched by increases in the yield of **I**, showing that the interaction with the second cytochrome *c* leads to et. As with Cc(F), the et intermediate so produced dissociates slowly (Figure 3), indicating that the second cytochrome again is involved in a well-defined binding interaction. In short, we infer that (ZnP)CcP binds both Fe^{3+}Cc(F) and Fe^{3+}Cc(horse) with a 2:1 stoichiometry at two sites with very different affinities.

However, the fungal and horse cytochromes *c* show one distinct difference during titrations of (ZnP)CcP with Fe^{3+}Cc: **[I]** increases synchronously with k_q for Cc(horse), whereas it lags k_q for Cc(F). This difference is mirrored in complementary experiments where the complex is dissociated by raising the ionic strength (Figure 8): for Cc(horse), k_q and **[I]** change synchronously as μ increases, but for Cc(F) the loss of quenching lags the decrease in **[I]** as μ increases. The response of the complex with Cc(F) to KCl further demonstrates that site 2 is more sensitive to ionic strength than site 1.

As noted above, the results imply that quenching is by electron transfer when Fe^{3+}Cc(F) is bound at site 2 of ^{3}(ZnP)CcP, whereas when Fe^{3+}Cc(F) is bound at site 1 of ^{3}(ZnP)CcP, quenching is predominantly by a nonredox mechanism (presumably Förster energy transfer; Table II). In contrast, the synchrony in the behaviors of k_q and **[I]** for Cc(horse) indicates that electron transfer is the primary mode of quenching by Fe^{3+}Cc(horse) at *both* sites, i.e., that $^1k_Q \approx {}^1k_t$ and $^2k_Q \approx {}^2k_t$. It does appear that ^{3}(ZnP)CcP → Fe^{3+}Cc et is more efficient at site 2 than at site 1 for Cc(horse), just as it is for Cc(F). This can be seen by considering the titration with Fe^{3+}Cc(horse) in 10 mM KP_i (pH 7) (Figure 4B), for which $^1k_Q = 27\ s^{-1}$ and $k_s = {}^2k_Q/{}^2K_d = 0.5\ \mu M^{-1}\ s^{-1}$ (Table I). Simulations generated using eq 4 show that, for titrations of 5 μM peroxidase with 0–50 μM Cc, the curvature in the binding profiles becomes very difficult to detect when $K_d \geq 100\ \mu M$. Setting a lower limit of 100 μM on ^2K_d, we obtain ^2k_Q ($\approx {}^2k_t$) ≥ 54 s^{-1}, or no less than twice the value of ^1k_Q ($\approx {}^1k_t$), given above. This at least partially explains the species-dependent response of k_q to changes in solvent composition and temperature reported earlier (Nocek *et al.*, 1991), since different modes of quenching were being monitored for Cc(vertebrate) and Cc(F) at site 1. In particular, the cooperative conformational transition observed at low temperature probably reflects a change in the rate constant for energy transfer.[8]

The present work provides the definitive demonstration of 2:1 binding of Cc by CcP, but the first observations of a 2:1 binding stoichiometry came from Kang *et al.* (1977). The biphasic steady-state kinetics observed with eukaryotic cytochromes *c* at low μ was attributed to reaction at two distinct sites on the peroxidase, on the basis of the similarities of the apparent K_M values for the two kinetic phases and the K_d values measured by the Hummel and Dreyer (1962) gel-filtration procedure. Kang *et al.* (1977) further noted that the presence of an Fe^{3+}Cc at the high-affinity site leads to increased activity at the low-affinity site, suggesting an allosteric interaction between the two sites. More recently, it was confirmed that CcP binds two molecules of Cc at low ionic strength (Kornblatt & English, 1986).

The conclusion that a low-affinity site can bind Cc leads to the question of its location on the CcP molecule. It has been generally accepted that CcP strongly binds one molecule of Cc tightly at a site in the general region of the CcP surface first identified by Poulos and Kraut (1980) or perhaps at the different, but overlapping site seen in the cocrystal (Pelletier & Kraut, 1992), but with the proviso that multiple binding orientations must exist, as evidenced by instances of gated electron transfer (Hazzard *et al.*, 1988a,b; Wallin *et al.*, 1991). There is no experimental evidence yet as to the location of this site 2, but electrostatics simulations suggest that the best candidate is the area around Asp-150 of CcP (Northrup *et al.*, 1988; Northrup & Thomasson, 1992). Northrup and Thomasson find that binding of Cc to this low-affinity site is *electrostatically* favorable, even when another Cc molecule already occupies the high-affinity site.[9]

The above discussion has ignored the fact that Cc can bind to several redox states of CcP and that this binding might change with the state. (MP)CcP (M = Zn, Mg) contains a pentacoordinate M^{2+} protoporphyrin IX and thus is structurally and electrostatically equivalent to Fe^{2+}CcP.[10] In particular, it does not suffer from any perturbation of the protein binding surface, as might be caused by the common approach of attaching a reporter group or redox center to the surface. To assess the relationship between the results presented here and those expected for other states of the enzyme, let us recall that Fe^{2+}CcP and CcP-II(Fe^{4+}=O) have

[8] The absence of energy-transfer quenching by Fe^{3+}Cc(horse) at site 1 or by either type of Cc at site 2 is addressed in detail in a forthcoming paper on Förster energy transfer quenching of ^{3}(ZnP)CcP by Fe^{3+}Cc (J. M. Nocek and B. M. Hoffman, unpublished results).

[9] Upon consideration of the large hydrophobic and entropic terms that oppose each other, these authors concluded that a 2:1 complex is not stable at pH 6.

[10] The isomorphism of hemoglobin with Fe^{2+} and Mg^{2+} incorporated into the protein prove this point (Kuila *et al.*, 1991).

the same charge, whereas Fe^{3+}*Cc*P has an additional positive charge, as does *Cc*P-I, provided that Trp-191 is in the cation radical state. Thus, on the simplest electrostatic grounds, the present data for binding of Fe^{3+}*Cc* would apply directly to Fe^{2+}*Cc*P and *Cc*P-II(Fe^{4+}=O), and one might expect slightly weaker binding for Fe^{3+}*Cc*P and *Cc*P-I. Conversely, the binding in the et intermediate, I, would correspond to the binding of Fe^{2+}*Cc* by Fe^{3+}*Cc*P *and* *Cc*P-I, the latter of course representing a physiologically active complex. On this simplified basis, *Cc* with an attached tripositive ruthenium ion (Geren *et al.*, 1991; Hahm *et al.*, 1992) should have greatly increased binding to any of the states of the peroxidase as compared to native *Cc*. However, all such considerations must be tempered given the apparent importance of interprotein hydrophobic contacts (Pelletier & Kraut, 1992). Furthermore, there may well be functionally significant conformational differences among the redox states of *Cc*P. Such appears to be the case for *Cc*; Hake *et al.* (1992) found that Fe^{2+}*Cc* binds more tightly to Fe^{3+}*Cc*P than does Fe^{3+}*Cc*, even though the reverse would be expected on the basis of charge.

Dissociation Rate Constants. Figures 1 and 2 suggest that Fe^{3+}*Cc* and Fe^{2+}*Cc* dissociate from the peroxidase with very different rate constants, making it essential to reexamine these results in terms of the two binding sites on *Cc*P. Consider first measurements that apply only to the high-affinity site of the peroxidase; since ${}^1K_d \ll {}^2K_d$, this holds for *Cc*/*Cc*P < 1. For *Cc*(F:*Pm*), it was shown (Figure 2C) that the rate constant for dissociation of Fe^{3+}*Cc* from site 1, ${}^1k_{off}(3+)$, falls within the well-defined range of $20 < {}^1k_{off}(3+) < 200\ s^{-1}$ at low μ ($1 \le [P_i] \le 10$ mM), but that ${}^1k_{off}(3+) > 200\ s^{-1}$ when $[P_i] \ge 50$ mM (Figure 2D); these limits hold for all fungal *Cc*'s, including Fe^{3+}*Cc*(F:*Ck*) and Fe^{3+}*Cc*(F:iso-1). In contrast, the exponential ^{3}(MgP)*Cc*P decays, shown in Figure 2B, set only a lower limit on ${}^1k_{off}(3+)$ for *Cc*(horse) of ${}^1k_{off}(3+) > k_{obs} \approx 50\ s^{-1}$ in buffers with $[P_i] \ge 1$ mM. However, it must be noted that NMR measurements set a much larger lower limit of $1100\ s^{-1}$ for this cytochrome at low μ (Satterlee *et al.*, 1987). Because the binding of Fe^{3+}*Cc* to site 1 of *Cc*P is much stronger than to site 2, it is reasonable to expect that dissociation is more rapid from site 2, namely, that ${}^2k_{off}(3+) \gg {}^1k_{off}(3+)$. With the reasonable estimates of $k_{on} = 10^8\ M^{-1}\ s^{-1}$ (Kim *et al.*, 1990) and ${}^2K_d \ge 100\ \mu M$, one calculates that ${}^2k_{off}(3+) \ge 10^4\ s^{-1}$. Indeed, that horse and fungal Fe^{3+}*Cc* bound to (MP)*Cc*P at site 2 are in rapid equilibrium is confirmed by experiment. For all *Cc* in buffers with $[P_i] > 1$ mM, the ^{3}(MP)*Cc*P decays are exponential at high *Cc*/*Cc*P, whereas slow dissociation from site 2 would lead to a biexponential decay with the two rate constants corresponding to the decays of the 1:1 and 2:1 complexes, respectively.

Consider now the dissociation rate constant for Fe^{2+}*Cc*. Because ^{3}(ZnP)*Cc*P → Fe^{3+}*Cc* et is more efficient in the 2:1 complex, the limit ${}^2k_{off}(2+) < 10\ s^{-1}$ set by the shape of the I progress curve (Figure 3) thus applies to Fe^{2+}*Cc* bound at site 2 in a 2:1 complex. The observation that ${}^2k_{off}(2+) \ll {}^2k_{off}(3+)$ is consistent with efficient release of product during the catalytic cycle. While the quantitative difference in dissociation rate constants for Fe^{2+}*Cc* and Fe^{3+}*Cc* seems surprisingly large in light of other binding studies[11] (Leonard & Yonetani, 1974; Vitello & Erman, 1987; Corin *et al.*, 1991; Hake *et al.*, 1991), the trend agrees with a recent binding study utilizing a cytochrome *c* affinity column, which found that *Cc*P binds 50 times more tightly to Fe^{2+}*Cc* than to Fe^{3+}*Cc* (Hake *et al.*, 1992). These differences are being investigated further.

Mechanistic Implications for a One-Site Catalytic Mechanism. From the response of the 2:1 complex of (ZnP)*Cc*P and Fe^{3+}*Cc*(F:*Pm*) to increasing [KCl] (Figure 8), it is evident that, in these experiments, site 2 is almost completely dissociated for $\mu \ge 50$ mM. However, this does not preclude functional significance for this low-affinity site at physiological μ (150–200 mM), because the proteins are quite dilute under our conditions, and the concentration of *Cc* in the intermembrane space is likely to be as high as 500 μM (Osheroff *et al.*, 1978), driving the equilibrium toward complex formation. In all considerations of enzymic activities it must not be overlooked that the physiological concentrations of components *in vivo* are orders of magnitude higher than those employed in typical *in vitro* studies. Nevertheless, reaction at site 2 need not require formation of the 2:1 complex. The high-affinity site could serve to "recruit" a *Cc* that subsequently migrates to site 2, either by surface diffusion or by dissociation and reassociation, in what might be termed a "bait and switch" mechanism. In either case, the increased *local* concentration of *Cc* associated with binding to site 1 will enhance the probability that a *Cc* will interact at site 2.

The present results further offer a possible explanation for an apparent contradiction in the steady-state kinetics. Erman *et al.* (1991) report that the maximum turnover rates (TN_{max}) for the steady-state, *Cc*P-catalyzed reduction of H_2O_2 by Fe^{2+}*Cc*(horse) and Fe^{2+}*Cc*(F:iso-1) in 4.2 mM KP_i (pH 7.5) are 290 and $780\ s^{-1}$, respectively. For *Cc*(horse), we find that ${}^1k_{off}(3+) > k_{obs} \approx 50\ s^{-1}$ under all conditions, and NMR studies yield ${}^1k_{off}(3+) \ge 1100\ s^{-1}$ (Satterlee *et al.*, 1987), results which are all consistent with a mechanism where product (Fe^{3+}*Cc*(horse)) dissociation from the high-affinity site is not rate-limiting. However, for *Cc*(F) in buffers where $1 \le [P_i] \le 10$ mM, we see that ${}^1k_{off}(3+)$ is $<200\ s^{-1}$ for *Cc*(F), which is consistent with the upper limit of $670\ s^{-1}$ obtained by NMR for the k_{off} of Fe^{3+}*Cc*(F:iso-1) bound to Fe^{3+}*Cc*P in 10 mM KNO_3 (pH ~6.5) (Moench *et al.*, 1992). Our limit on ${}^1k_{off}(3+)$ clearly is much less than the $TN_{max} \approx 780\ s^{-1}$ for *Cc*(F:iso-1) in low ionic strength phosphate buffers and is *not* consistent with reaction of *Cc*(F) solely at site 1 of *Cc*P under these conditions. Each cycle of H_2O_2 reduction requires the reaction of *Cc*P with two *Cc* (Scheme I, eq 1) and thus two separate steps of Fe^{3+}*Cc* dissociation. As ${}^1k_{off}(3+) < 200\ s^{-1}$ for *Cc*(F:iso-1), even a single product dissociation step would be rate-limiting in a one-site mechanism. However, reaction of *Cc*(F:iso-1) at site 2, where ${}^2k_{off}(3+)$ is large (Table I), obviously could account for the high turnover.

There are other indications that the low-affinity site is essential for the activity of the native enzyme. Measurements of steady-state velocity and et rates versus [*Cc*(F:iso-1)] (Erman *et al.*, 1991) would lead to dissociation constants that increase with decreasing ionic strength: $K_d = 2.0\ \mu M$ at $\mu = 100$ mM, but $K_d = 150\ \mu M$ at $\mu = 10$ mM, if analyzed within a one-site model.[12] Such an ionic strength dependence is inconsistent with electrostatically driven, one-site binding, and the data can be interpreted instead as reflecting the presence of two binding sites. The K_d value at $\mu = 100$ mM agrees well with the ${}^1K_d \approx 1.4\ \mu M$ seen for *Cc*(F:iso-1) in 50 mM KP_i (pH 7) ($\mu \approx 90$ mM) (Figure 3A) and so at this ionic strength probably represents 1:1 binding to site 1 of the peroxidase. However, just as Fe^{2+}*Cc* → *Cc*P-I et is inhibited at low μ

[11] It is worth noting that, while our observation applies only to the low-affinity site of *Cc*P, these studies detected only 1:1 binding and thus probably only apply to the high-affinity site.

[12] These authors clearly recognize this inconsistency and denote their values as "apparent" dissociation constants (Erman *et al.*, 1991).

(Hazzard *et al.*, 1988a,b) so might the binding to site 1 be too tight for efficient enzyme turnover under such conditions, as found by Kang *et al.* (1977). The apparent K_d of 150 μM seen at μ = 10 mM by Erman *et al.* (1991) instead probably reflects the binding of Cc(F:iso-1) to site 2 of CcP to form a 2:1 complex. We saw a result similar to this in the titration of (ZnP)CcP with Fe^{3+}Cc(horse) in 1 mM KP_i (pH 7) (Figures 5B and 9B). In summary, both the (ZnP)CcP data and the kinetics of the native enzyme suggest that the low-affinity site on CcP is catalytically active.

Two Binding Sites for Two Redox Sites? The conclusion that CcP binds Cc at two distinct sites naturally leads to the question of whether or not an individual binding site supports preferential reduction by Fe^{2+}Cc of one of the two redox-active centers of CcP-I. Recall that, in low ionic strength buffers, only 1:1 complex is formed when Cc/CcP < 1, with Cc bound at the high-affinity site of CcP, whereas some 2:1 complex is formed when Cc/CcP > 1. Stopped-flow titrations of CcP-I with Fe^{2+}Cc(horse) at low ionic strength (Summers & Erman, 1988) show that Trp-191· is reduced preferentially to the (Fe^{4+}=O) heme when Cc/CcP < 1, but that this order is reversed at higher values of Cc/CcP.[13] In flash photolysis studies of 1:1 complexes of CcP-I with ruthenium-modified cytochromes at low μ (Geren *et al.*, 1991; Hahm *et al.*, 1992), Millett and co-workers clearly observe direct reduction of the Trp-191· radical with a large rate constant, typically $>10^4$ s^{-1}, followed by a slower reduction of the remaining (Fe^{4+}=O) heme in CcP-II, with a rate constant of $\sim 10^2$ s^{-1}. Taken together with our findings of relatively inefficient zinc porphyrin to heme et at site 1 of (ZnP)CcP, these results suggest that et events at site 1 favor reduction of the radical, while et at site 2 is optimized for reduction of the oxyferryl heme. Indeed, as noted above, such a hypothesis of distinct binding sites for each of the two oxidizing equivalents in the peroxidase was first presented by Margoliash and co-workers (Kang *et al.*, 1977).

The et pathway from the Cc heme to the CcP heme (Beratan *et al.*, 1992) proposed for the recent X-ray (Pelletier & Kraut, 1992) structure of the complex travels through Trp-191. As we consider the cocrystal binding site and that in the Poulos–Kraut model to be part of the same high-affinity binding domain (Figure 10), this pathway is consistent with the observed direct reduction of Trp-191· (Geren *et al.*, 1991; Hahm *et al.*, 1992) and the proposal above that et at site 1 favors reduction of the radical, since the electron must travel through this residue *en route* to the CcP heme. However, the suggestion of two sites for two equivalents seems inconsistent with the extremely low steady-state activity of the Trp-191 → Phe mutant (Mauro *et al.*, 1988) of the recombinant peroxidase, CcP(MI), since et at the low-affinity site should favor reduction of the oxyferryl heme and not the radical. Asp-152, an acidic surface residue thought to be within the low-affinity binding site, is changed to Gly in the recombinant peroxidase, but the influence of this substitution on the reactivity of the low-affinity site remains to be determined. It is also possible that the structural perturbations in this mutant disrupt the heme–heme et at site 2, perhaps by changing some key hydrogen bonds in an otherwise efficient et pathway. Clearly, resolution of this issue will require further efforts using multiple experimental approaches.

[13] Interestingly, Summers and Erman (1988) concluded that et from Fe^{2+}Cc to Trp-191· is not direct but rather proceeds through the heme, with an intramolecular electron transfer leading to formation of the more thermodynamically stable form of compound II, CcP-II(Fe^{4+}=O).

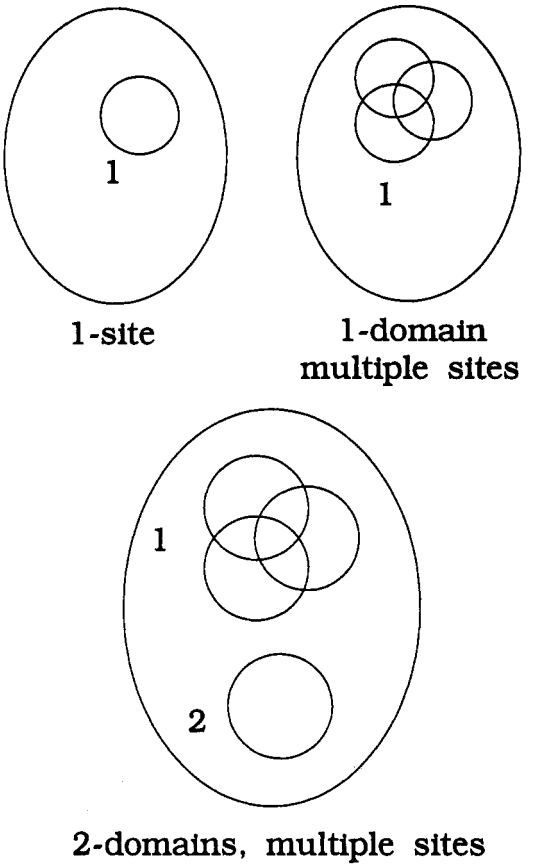

FIGURE 10: Binding schemes for CcP. Schematic representations of (i) 1:1 binding of Cc by CcP at a single discrete binding site, (ii) 1:1 binding of Cc by CcP at a domain with three overlapping sites, and (iii) 2:1 binding of Cc by CcP at two distinct binding domains.

Our titrations of (ZnP)CcP predict that, even with site 1 occupied, site 2 should be available and capable of efficient et. Thus it is somewhat perplexing to us that 1:1 covalent complexes containing the native enzyme exhibit poor reactivity with exogenous Fe^{2+}Cc (Erman *et al.*, 1987; Waldmeyer & Bosshard, 1985). This could be due to the modification of carboxylates in the low-affinity binding domain by the cross-linking reagent. However, if we assume that the binding surface of CcP is uncorrupted in these covalent complexes, another possible explanation is that site 2 is not the location of the et event and that enhanced activity of a 2:1 complex relative to a 1:1 complex is due to a positive allosteric interaction triggered by binding of the second cytochrome. In fact, modulation of CcP activity at one site through binding of Cc at another site has been previously proposed (Kang *et al.*, 1977). At present, we prefer the simpler and more direct interpretation of et occurring at site 2, but further studies are required to firmly decide these issues.

CONCLUSIONS

In this report, we showed that, at low ionic strength, (ZnP)CcP binds two molecules of Fe^{3+}Cc at two distinct sites with different affinities (Table II) and that ^{3}(ZnP)CcP → Fe^{3+}Cc et is far more efficient at the lower affinity site. When bound at the high-affinity site, Fe^{3+}Cc(F) strongly quenches ^{3}(ZnP)CcP, but it does so predominantly by a nonredox mechanism (presumably Förster energy transfer). In contrast,

[14] For concreteness, we depict *four* sites to be consistent with the four binding minima found for Cc on the CcP surface by electrostatics calculations (Northrup *et al.*, 1988).

Fe^{3+}C*c*(horse) bound to this site quenches ^{3}(ZnP)C*c*P less efficiently than Fe^{3+}C*c*(F), and apparently only by electron transfer. For both types of Fe^{3+}C*c*, binding to the low-affinity site is more sensitive to ionic strength than binding to the high-affinity site. When bound to the high-affinity site in a 1:1 complex, k_{off} for Fe^{3+}C*c*(F) is $<200\ s^{-1}$ at low ionic strength but $>200\ s^{-1}$ at high ionic strength; for Fe^{3+}C*c*(horse), $k_{off} > 50\ s^{-1}$ under all buffer conditions. The dissociation rate constant is strongly dependent upon the cytochrome oxidation state, with Fe^{2+}C*c* binding more tightly than Fe^{3+}C*c*. These points are presented again in Table II.

These findings may be profitably placed in a historical perspective (Salemme, 1993). The earliest efforts at modeling protein–protein complexes were performed in the face of severe computational limitations. The finding of electrostatically complementary surfaces on electron-transfer partners such as cytochrome b_5 (b_5) and C*c* (Salemme, 1976) and C*c*P and C*c* (Poulos & Kraut, 1980), as well as b_5 and hemoglobin (Mauk & Mauk, 1982), led to pictures of docked complexes that naturally dominated the thinking about such complexes and perhaps inevitably promoted a picture of protein partners specifically docked in a static 1:1 diprotein complex, reminiscent of the lock-and-key motif for enzyme–substrate interactions (Stryer, 1988). Indeed, early studies of the C*c*P–C*c* complex in solution (Waldmeyer & Bosshard, 1985; Bechtold & Bosshard, 1985; Satterlee *et al.*, 1987) generally supported the one-site model of Poulos and Kraut (1980) (Figure 10, upper left). However, the observation of gated electron transfer in several kinetic investigations (Hazzard *et al.*, 1988a,b; Wallin *et al.*, 1991) shows that the 1:1 complex is dynamic, sampling several orientations during an encounter (Northrup *et al.*, 1988), and that the docking geometry may depend upon the oxidation state of the cytochrome (McLendon *et al.*, 1991; Hake *et al.*, 1992). Indeed, if solution studies may be taken to support the existence of a Poulos–Kraut complex, then direct evidence for different dockings is provided by the recent crystal structure of the complex: the binding sites in the computer model (Poulos & Kraut, 1980) and the cocrystal (Pelletier & Kraut, 1992) are different but overlapping, because at least one close contact, C*c*P(Asp-34): C*c*(Lys-87), is present in both. Such observations naturally lead to a picture of a high-affinity binding *domain* on C*c*P with multiple, overlapping *sites* for C*c* (Figure 10, upper right) (McLendon, 1991).

Our results extend rather than contradict such findings of strong, yet dynamic, binding of this kind by indicating that, when $Cc/CcP > 1$, one must include a second distinct binding domain. Thus, our findings of 2:1 binding stoichiometry at low μ then lead to a schematic model of the peroxidase with *both* (1) a high-affinity domain containing several, overlapping sites and (2) a low-affinity domain, as shown in the bottom of Figure 10.[14] The existence of multiple sites in the low-affinity domain is possible and even likely, but is not necessary to explain our results.

We have clearly demonstrated the potential for a highly reactive, low-affinity site to perform an essential role in electron transfer and in catalysis *in vivo*. The confirmation of a 2:1 C*c*–C*c*P binding stoichiometry, coupled with the observation of et activity from C*c* bound at the low-affinity site, clearly demonstrates the need to reevaluate previous studies of this enzyme which assumed that only the 1:1 complex is formed or that electron transfer occurs only at the high-affinity site. Specifically at issue is any study whose interpretation scheme assumed a 1:1 stoichiometry, yet where the experiments were performed at low ionic strength with $Cc/CcP > 1$ and/or at high protein concentrations; future studies of C*c*P must consider more seriously the implications of this low-affinity site on C*c*P. Finally, from a more general perspective, it is apparent that the fact that an enzyme binding site has low affinity for substrate does not preclude it having significant reactivity. Certainly, the possibility of several et-active binding sites should be explored fully for other et proteins, particularly those with multiple redox centers.

ACKNOWLEDGMENTS

We are indebted to Dr. Judy Nocek for helpful discussions and for writing the computer programs used to fit the binding profiles. We further thank Prof. Emanuel Margoliash for a careful reading of the manuscript prior to submission, Prof. A. Grant Mauk for providing the recombinant iso-1 cytochrome *c*, Prof. Irving Klotz for a series of lectures on ligand–receptor interactions, and Prof. Scott Northrup for communicating results prior to publication. These experiments were presented in preliminary form at the 205th National Meeting of the American Chemical Society, Denver, CO, May 1993.

REFERENCES

Bechtold, R., & Bosshard, H. R. (1985) *J. Biol. Chem. 260*, 5191–5200.

Beratan, D. N., Onuchic, J. N., Winkler, J. R., & Gray, H. B. (1992) *Science 258*, 1740–1741.

Berg, O. G., & von Hippel, P. H. (1985) *Annu. Rev. Biophys. Biophys. Chem. 14*, 131–160.

Bosshard, H. R., Anni, H., & Yonetani, T. (1991) in *Peroxidases in Chemistry and Biology* (Everse, J., Everse, K. E., & Grisham, M. B., Eds.) Vol. 2, Chapter 3, pp 52–78, CRC Press, Boca Raton, FL.

Brautigan, D. L., Ferguson-Miller, S., & Margoliash, E. (1978) *Methods Enzymol. 53*, 128–164.

Corin, A. F., McLendon, G., Zhang, Q., Hake, R. A., Falvo, J., Lu, K. S., Ciccarelli, R. B., & Holzschu, D. (1991) *Biochemistry 30*, 11585–11595.

Cutler, R. L., Pielak, G. J., Mauk, A. G., & Smith, M. (1987) *Protein Eng. 1*, 95–99.

Dixon, D. W., Hong, X., & Woehler, S. E. (1989) *Biophys. J. 56*, 339–351.

English, A. M., Laberge, M., & Walsh, M. (1986) *Inorg. Chim. Acta 123*, 113–116.

Erman, J. E., & Vitello, L. B. (1980) *J. Biol. Chem. 255*, 6224–6227.

Erman, J. E., Kim, K. L., Vitello, L. B., Moench, S. J., & Satterlee, J. D. (1987) *Biochim. Biophys. Acta 911*, 1–10.

Erman, J. E., Kang, D. S., Kim, K. L., Summers, F. E., Matthis, A. L., & Vitello, L. B. (1991) *Mol. Cryst. Liq. Cryst. 194*, 253–258.

Everest, A. M., Wallin, S. A., Stemp, E. D. A., Nocek, J. M., Mauk, A. G., & Hoffman, B. M. (1991) *J. Am. Chem. Soc. 113*, 4337–4338.

Finzel, B. C., Poulos, T. L., & Kraut, J. (1984) *J. Biol. Chem. 259*, 13027–13036.

Geren, L., Hahm, S., Durham, B., & Millett, F. (1991) *Biochemistry 30*, 9450–9457.

Gupta, R. K., & Yonetani, T. (1973) *Biochim. Biophys. Acta 292*, 502–508.

Hahm, S., Durham, B., & Millett, F. (1992) *Biochemistry 31*, 3472–3477.

Hake, R., Zhang, Q., Marohn, J., McLendon, G., & Corin, A. (1991) *Mol. Cryst. Liq. Cryst. 194*, 351–356.

Hake, R., McLendon, G., Corin, A., & Holzschu, D. (1992) *J. Am. Chem. Soc. 114*, 5442–5443.

Hazzard, J. T., McLendon, G., Cusanovich, M. A., Das, G., Sherman, F., & Tollin, G. (1988a) *Biochemistry 27*, 4445–4451.

Hazzard, J. T., Moench, S. J., Erman, J. E., Satterlee, J. D., & Tollin, G. (1988b) *Biochemistry 27*, 2002–2008.
Ho, P. S., Hoffman, B. M., Kang, C. H., & Margoliash, E. (1983) *J. Biol. Chem. 258*, 4356–4363.
Ho, P. S., Hoffman, B. M., Solomon, N., Kang, C. H., & Margoliash, E. (1984) *Biochemistry 23*, 4122–4128.
Ho, P. S., Sutoris, C., Liang, N., Margoliash, E., & Hoffman, B. M. (1985) *J. Am. Chem. Soc. 107*, 1070–1071.
Hoffman, B. M., & Ratner, M. R. (1987) *J. Am. Chem. Soc. 109*, 6237–6243.
Hoffman, B. M., Ratner, M. A., & Wallin, S. A. (1990) in *Advances in Chemistry Series* (Johnson, M. K., King, R. B., Kurtz, D. M., Jr., Kutal, C., Norton, M. L., & Scott, R. A., Eds.) Vol. 226, Chapter 6, pp 125–146, American Chemical Society, Washington, D.C.
Hoffman, B. M., Natan, M. J., Nocek, J. M., & Wallin, S. A. (1991) *Struct. Bonding 75*, 85–108.
Hummel, J. P., & Dreyer, W. J. (1962) *Biochim. Biophys. Acta 63*, 530–532.
Kang, C. H., Ferguson-Miller, S., & Margoliash, E. (1977) *J. Biol. Chem. 252*, 919–926.
Kim, K. L., Kang, D. S., Vitello, L. B., & Erman, J. E. (1990) *Biochemistry 29*, 9150–9159.
Klotz, I. M. (1985) *Q. Rev. Biophys. 18*, 227–259.
Klotz, I. M., & Hunston, D. L. (1979) *Arch. Biochem. Biophys. 193*, 314–328.
Kornblatt, J. A., & English, A. M. (1986) *Eur. J. Biochem. 155*, 505–511.
Kuila, D., Natan, M. J., Rogers, P., Gingrich, D. J., Baxter, W. W., Arnone, A., & Hoffman, B. M. (1991) *J. Am. Chem. Soc. 113*, 6520–6526.
Leonard, J. J., & Yonetani, T. (1974) *Biochemistry 13*, 1465–1468.
Liang, N., Kang, C. H., Ho, P. S., Margoliash, E., & Hoffman, B. M. (1986) *J. Am. Chem. Soc. 108*, 4665–4666.
Liang, N., Mauk, A. G., Pielak, G. J., Johnson, J. A., Smith, M., & Hoffman, B. M. (1988) *Science 240*, 311–313.
Luchi, J., & Hoffman, B. M. (manuscript in preparation).
Margoliash, E., & Frohwirt, N. (1959) *Biochem. J. 71*, 570–572.
Mauk, M. R., & Mauk, A. G. (1982) *Biochemistry 21*, 4730–4734.
Mauro, J. M., Fishel, L. A., Hazzard, J. T., Meyer, T. E., Tollin, G., Cusanovich, M. A., & Kraut, J. (1988) *Biochemistry 27*, 6243–6526.
McLendon, G. (1991) *Struct. Bonding 75*, 159–174.
McLendon, G., & Hake, R. (1992) *Chem. Rev. 92*, 481–490.
McLendon, G., Hake, R., Zhang, Q., & Corin, A. (1991) *Mol. Cryst. Liq. Cryst. 194*, 225–232.
Mochan, E. (1970) *Biochim. Biophys. Acta 216*, 80–95.
Mochan, E., & Nicholls, P. (1971) *Biochem. J. 121*, 69–82.
Moench, S. J., Chroni, S., Lou, B.-S., Erman, J. E., & Satterlee, J. D. (1992) *Biochemistry 31*, 3661–3670.
Nelson, C. E., Sitzman, E. V., Kang, C. H., & Margoliash, E. (1977) *Anal. Biochem. 83*, 622–631.
Nocek, J. M., Stemp, E. D. A., Finnegan, M. G., Koshy, T. I., Johnson, M. K., Margoliash, E., Mauk, A. G., Smith, M., & Hoffman, B. M. (1991) *J. Am. Chem. Soc. 113*, 6822–6831.
Northrup, S. H., & Thomasson, K. A. (1992) *FASEB J. 6*, A474.
Northrup, S. H., Boles, J. O., & Reynolds, J. C. L. (1988) *Science 241*, 67–70.
Osheroff, N., Koppenol, W. H., & Margoliash, E. (1978) in *Frontiers of Biological Energetics* (Scarpa, A., Dutton, P. L., & Leigh, J. S., Eds.) pp 439–449, Academic Press, New York.
Peerey, L. M., Brothers, H. M., II, Hazzard, J. T., Tollin, G., & Kostic, N. M. (1991) *Biochemistry 30*, 9297–9304.
Pelletier, H., & Kraut, J. (1992) *Science 258*, 1748–1755.
Pettigrew, G. W., & Moore, G. R. (1987) *Cytochromes c: Biological Aspects*, Springer-Verlag, Berlin.
Poulos, T. L., & Kraut, J. (1980) *J. Biol. Chem. 255*, 10322–10330.
Poulos, T. L., Freer, S. T., Alden, R. A., Edwards, S. L., Skogland, U., Takio, K., Eriksson, B., Xuong, N., Yonetani, T., & Kraut, J. (1980) *J. Biol. Chem. 255*, 575–580.
Salemme, F. R. (1976) *J. Mol. Biol. 102*, 563–568.
Salemme, F. R. (1993) *Abstracts of Papers*, 205th National Meeting of the American Chemical Society, Denver, CO, May 1993, INOR 568, American Chemical Society, Washington, D.C.
Satterlee, J. D., Moench, S. J., & Erman, J. E. (1987) *Biochim. Biophys. Acta 912*, 87–97.
Simolo, K. P., McLendon, G. L., Mauk, M. R., & Mauk, A. G. (1984) *J. Am. Chem. Soc. 106*, 5012–5013.
Sivaraja, M., Goodin, D. B., Smith, M., & Hoffman, B. M. (1989) *Science 245*, 738–740.
Smulevich, G., Mantini, A. R., English, A. M., & Mauro, J. M. (1989) *Biochemistry 28*, 5058–5064.
Stemp, E. D. A., Nocek, J. M., Wallin, S. A., Siegel, D., Mansueto, L., & Hoffman, B. M. (manuscript in preparation).
Stryer, L. (1988) in *Biochemistry*, 3rd ed. Chapter 17, pp 397–426, W. H. Freeman and Company, New York.
Summers, F. E., & Erman, J. E. (1988) *J. Biol. Chem. 263*, 14267–14275.
Swanson, R., Trus, B. L., Mandel, N., Mandel, G., Kallai, O. B., & Dickerson, R. E. (1977) *J. Biol. Chem. 252*, 759–775.
Turro, N. J. (1978) *Modern Molecular Photochemistry*, pp 247–248, Bemjamin Cummings, Menlo Park, CA.
Vitello, L. B., & Erman, J. E. (1987) *Arch. Biochem. Biophys. 258*, 621–629.
Vitello, L. B., Huang, M., & Erman, J. E. (1990) *Biochemistry 29*, 4283–4288.
Waldmeyer, B., & Bosshard, H. R. (1985) *J. Biol. Chem. 260*, 5184–5190.
Wallin, S. A., Stemp, E. D. A., Everest, A. M., Nocek, J. M., Netzel, T. L., & Hoffman, B. M. (1991) *J. Am. Chem. Soc. 113*, 1842–1844.
Willie, A., Stayton, P. S., Sligar, S. G., Durham, B., & Millett, F. (1992) *Biochemistry 31*, 7237–7242.
Yonetani, T. (1967) *J. Biol. Chem. 242*, 5008–5013.
Yonetani, T. (1976) in *The Enzymes* (Boyer, P. D., Ed.) Vol. 13, Chapter 6, pp 345–361, Academic Press, Orlando, FL.
Zhou, J. S., & Kostic, N. M. (1991) *J. Am. Chem. Soc. 113*, 6067–6073.
Zhou, J. S., & Kostic, N. M. (1992a) *J. Am. Chem. Soc. 114*, 3562–3563.
Zhou, J. S., & Kostic, N. M. (1992b) *Biochemistry 31*, 7543–7550.